

A Survey on Physical Adversarial Attack in Computer Vision

Donghua Wang^{1,2}, Wen Yao^{2*}, Tingsong Jiang^{2*}, Guijian Tang^{2,3}, Xiaoqian Chen²

¹ College of Computer Science and Technology, Zhejiang University, Hangzhou, China

² Defense Innovation Institute, Chinese Academy of Military Science, Beijing, China

³ College of Aerospace Science and Engineering, National University of Defense Technology, Changsha, China
wangdonghua@zju.edu.cn, wendy0782@126.com, tingsong@pku.edu.cn, tangbanlniu@163.com,
chenxiaoqian@nudt.edu.cn

Abstract—In the past decade, deep learning has dramatically changed the traditional hand-craft feature manner with strong feature learning capability, promoting the tremendous improvement of conventional tasks. However, deep neural networks (DNNs) have been demonstrated to be vulnerable to adversarial examples crafted by small noise, which is imperceptible to human observers but can make DNNs misbehave. Existing adversarial attacks can be divided into digital and physical adversarial attacks. The former is designed to pursue strong attack performance in lab environments while hardly remaining effective when applied to the physical world. In contrast, the latter focus on developing physical deployable attacks, which are more robust in complex physical environmental conditions (e.g., brightness, occlusion, etc.). Recently, with the increasing deployment of the DNN-based system in the real world, enhancing the robustness of these systems is an emergency, while exploring physical adversarial attacks exhaustively is the precondition. To this end, this paper reviews the development of physical adversarial attacks against DNN-based computer vision tasks (i.e., image recognition and object detection tasks), which can provide beneficial information for developing stronger physical adversarial attacks. For completeness, we will briefly introduce the works that do not involve physical attacks but are closely related to them. Specifically, we first proposed a taxonomy to summarize the current physical adversarial attacks. Then we briefly discuss the existing physical attacks and focus on the technique for improving the robustness of physical attacks under complex physical environmental conditions. Finally, we discuss the issues of the current physical adversarial attacks to be solved and give promising directions.

Index Terms—Adversarial examples, Physical adversarial attacks, Security of neural network

I. INTRODUCTION

DEEP neural networks (DNNs) achieves considerable success in a wide range of research filed, including computer vision [1]–[4], natural language processing [5], [6], and speech recognition [7], [8]. Applications with the core of these advanced techniques have been widely deployed in the real world, such as facial payment, medical image diagnosis, automatic driving, and so on. However, DNNs have exposed their security risks to adversarial examples crafted by small noises that are invisible to humane observers but can mislead the DNNs to output wrong results. For instance,

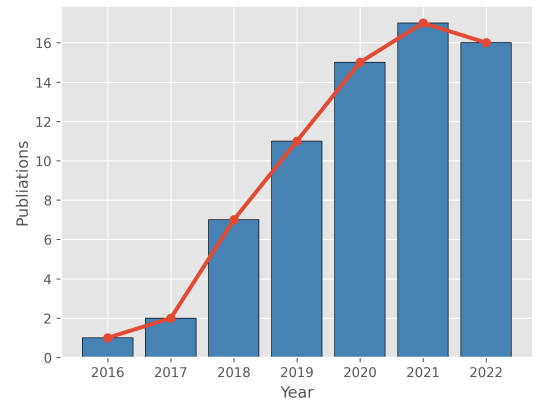


Fig. 1. Count of physical attack literature published yearly.

elaborately designed glasses frames can bypass the facial recognition system; the automatic driving car is susceptible to environmental changes (e.g., shadow or brightness), resulting in out-of-control or misdetection. That poses a potential risk for deploying DNN-based systems in the real world, especially for security-sensitive applications.

Since Szegedy *et al.* [9] first found that the DNN-based image classifier is susceptible to malicious devised noise, a line of works [10]–[16] have been proposed to explore the adversarial examples and the corresponding countermeasure techniques in different research areas, especially in computer vision. Accordingly, many surveys [17]–[22] were proposed to the taxonomy or summarize the development of the adversarial examples. Serban *et al.* [21] made taxonomy exhaustively for attack and systemically summarized the existing attack methods from machine learning to DNNs. [20], [22]–[25] reviewed the development of adversarial attack and defense methods against DNNs at different times. Some survey only focus on the specific task, such as image classification [26], adversarial patch [27]. However, these surveys mainly provide an overall view of the adversarial attack and defense in the specific research area or a roughly overall view. Moreover, with the increasingly maturing of DNNs in commercial deployment, exploring the physical attack is more urgent for enhancing the robustness of DNN-based systems. Although some works have reviewed the development of physical attacks [22], [28],

*Wen Yao and Tingsong Jiang are the corresponding authors.

they are out-of-date since plenty of novel physical attacks have emerged [29]–[39] in the past two years. Concurrent to our work, although [40], [41] review physical attacks, they only review some of the current physical attacks, i.e., 43 and 46 publications, respectively. In contrast, we review 69 publications on physical attacks. Figure 1 illustrates the number of physical attack literature published yearly since 2016. Therefore, it is necessary to analyze the newly proposed method for better tracking the latest research direction.

In this paper, we comprehensively review the existing physical adversarial attacks in the computer vision task. Given the statistical result of the current literature, we mainly survey the two most prevalent tasks: image recognition and object detection. Note that, object tracking and semantic segmentation tasks are similar to object detection. Thus we include the physical adversarial attack against object tracking and semantic segmentation in object detection. Specifically, we first propose a taxonomy to summarize the current physical adversarial attacks from the formal of adversarial perturbation, the way of physical attack, the settings of physical attack, and so on. Then, we briefly analyze different physical adversarial attacks in detail. After reviewing attacks for each field, we summarize the most frequently used technique for improving the robustness of physical attacks. Finally, we discuss the issues of the current physical adversarial attacks to be solved and the promising direction. We hope this survey will provide comprehensive retrospect and beneficial information on physical adversarial attacks for researchers.

To cover the existing physical attacks as much as possible, we searched the keywords “physical attack” or “physical adversarial examples” from Google Scholar to obtain the latest paper. In addition, conference proceedings in CVPR, ICCV, ECCV, AAAI, IJCAI, ICML, ICLR, and NeurIPS were searched based on the keyword toward titles of the papers. We manually checked the references in all selected papers to seek the relevant literature to avoid leakage. In addition, we exclude papers that have not relevant to physical adversarial attacks. Finally, we collected 69 physical adversarial attack papers in computer vision.

In summary, our contributions are listed as follows.

- We make a comprehensive survey on physical adversarial attacks in computer vision tasks to provide overall knowledge about this research field.
- We propose a taxonomy to summarize the existing physical adversarial attacks according to the characteristic of different attacks. We briefly discuss different physical attacks and outline the most frequently used techniques for improving the robustness of physical attacks.
- We discuss the challenging and research directions for physical adversarial attacks based on the following issues: input transformation augmentation; attack algorithm design consisting of developing physical attacks under black-box settings, transferability, attack multitask, and so on; evaluation contains physically attack benchmark evaluation datasets construction and uniform physical test criterion.

TERMINOLOGY	
x	Clean image.
y	Ground truth of the image.
\hat{x}	Clean image in the physical world.
x_{adv}	Adversarial example.
\hat{x}_{adv}	Adversarial example in the physical world.
δ	Adversarial perturbation.
ϵ	Maximum allowable magnitude of perturbation.
f	Neural network.
y_{cls}	Ground truth label for the classification task.
y_{obj}	Ground truth label for the object detection task.
$J_f(\cdot)$	Loss function for neural network f .
$\nabla J_f(\cdot)$	The gradient of the f with respect to the input x .
$\ \cdot\ _p$	L_p norm distance.
$d(\cdot, \cdot)$	Distance metrics.
\mathcal{T}	Transformation distribution.
t	A specific transformation.

II. FUNDAMENTAL CONCEPT

In this section, we briefly introduce the foundation concept of deep learning and adversarial examples.

A. Deep learning

Deep learning, a data-driven technique, is known for its powerful capability to understand data patterns and features from enormous data, where the learned representations are beneficial to various regressions or classification tasks. In general, the deep learning technique consists of data preprocessing, architecture design, training strategy, loss function, and performance metrics. The core component of deep learning is automatic feature learning driven by deep neural networks (DNNs), in which the most representative characteristic is that it can extract useful features from considerable data in an end-to-end manner.

The architecture of DNN is determined by the different connections and numbers between the neurons and the layers. In the past decade, convolutional neural networks (CNNs) were the most commonly used architecture in computer vision tasks and have been maturely deployed in commercial applications. CNN consists of multiple hidden layers with different connections, where each layer contains several convolution kernels for extracting different feature representations from input data. The representative architecture of CNN in computer vision is ResNet [2], VGG [42], and DenseNet [43], which are employed in image recognition tasks and object detection tasks [2], [44]. Recently, inspired by the incredible success of transformer architecture in the NLP task, the transformer has gradually been applied to computer vision tasks, called vision transformers. Vision transformer consists of an encoder and decoder with several transformer blocks of the same architecture. The encoder produces the embedding of the inputs, while the decoder takes all embedding as input to generate the output with their incorporated contextual information. Despite the architecture discrepancy between different networks, the neural network has a uniform representation formal, i.e., $f(x)$, and the concrete representation of $f(x)$ depends on the given tasks. However, despite DNNs achieving great success, the underlying mechanism of DNNs is unclear and exposing the potential security risks as it is overly dependent on the data.

B. Adversarial examples

The concept of the adversarial examples was first proposed by Szegedy *et al.* [9], which refers to a kind of sample containing carefully crafted noise that is invisible to human observers but can mislead the DNN to make the wrong output. Specifically, given an image x and a well-trained network f , the adversarial examples can be represented as the following optimization problem

$$\begin{aligned} \min \quad & \delta \\ \text{s.t.} \quad & f(x + \delta) \neq f(x) \\ & \|\delta\|_p \leq \epsilon, \end{aligned} \quad (1)$$

where the $\|\cdot\|_p$ is the L_p -norm, ϵ is the maximum magnitude of the δ under the constrain of L_p -norm. L_0 , L_2 and L_∞ are the three commonly used L_p metrics. L_0 counts the number of the non-zero pixels in the adversarial perturbation δ , L_2 measures the Euclidean distance between the δ and zero, and L_∞ measures the maximum value of δ .

Adversarial examples can be used to perform attacks on the digital world and the physical world. In digital world attacks, the adversary aims to explore corner cases that can fool the DNNs, where the optimization and evaluation settings are ideal and remain unchanged. By contrast, in physical world attacks, there is a huge gap between the optimization and evaluation of adversarial examples. The adversarial perturbation is usually generated in the digital world in advance and then required to be made out (e.g., printed out) at the attack stage. Therefore, the adversarial perturbation might encounter the following loss at the attack stage: on the first hand, loss caused by the device noise and color discrepancy between digital and physical caused by the printer. On the other hand, content distortion originated in complex environmental conditions, such as lighting, shadow, occlusion, brightness changing, rotation, deformation, and so on. Note that, despite some works attempting to attack the online employed DNN-based systems, we do not discuss these works as we are focused on the attacks that can apply to the real world. Based on the above discussion, developing effective physical adversarial attacks are more challenging than digital attacks.

III. TAXONOMY OF PHYSICAL ADVERSARIAL EXAMPLES

In this section, we propose a taxonomy scheme to systematically categorize the existing physical adversarial attack methods in computer vision tasks. Specifically, we first introduce the basic classification of adversarial examples. Then, we divide all physical adversarial attack methods in the computer vision tasks into image classification and object detection according to the tasks of victim models. We then categorize the existing physical attack methods in terms of the form of perturbation, the way of attacks, representative techniques for improving the robustness of physical attacks, and testing environments according to the implementation details of different attack methods. Finally, we describe three widely used techniques for improving physical attack strengths.

A. Adversary's knowledge

1) *White-box attacks*: White-box attacks assume the adversary has full knowledge about the target victim network, including architecture, parameters, and training data. In white-box settings, the adversary is permitted to exploit the gradient with respect to input images of the target victim model to construct the adversarial examples. Therefore, white-box attacks are the most efficient adversarial attacks at present.

2) *Black-box attacks*: Black-box attacks assume the adversary has no knowledge about the target victim network but allows the adversarial to query the target model, which makes it more suitable in practice. Therefore, black-box attacks are more challenging than white-box attacks. Nonetheless, there are some algorithms to perform black-box attacks, such as genetic algorithm, evolution evolution algorithm, and differential algorithm, or exploit the transferability of adversarial examples.

B. Adversarial specificity

1) *Non-targeted attack*: Non-targeted attacks mislead the target victim model to output any class except the original. Intuitively, non-target attacks tend to search the adversarial example along the direction of the nearest decision boundary to the original sample.

2) *Targeted attacks*: Targeted attacks refer to misleading the target victim model to output a pre-specific class. Although object detection has multiple outputs (i.e., bounding boxes, classes, and the confidence score of the detected object), it can be uniformly represented as the class in targeted attacks for consistency with classification tasks. Targeted attacks are hard to realize when the distance between the original class and the target class in the high-dimensional decision boundary is far. Therefore, targeted attacks are more challenging than non-targeted.

C. Computer vision tasks

1) *Image recognition task*: Image recognition is a conventional task in computer vision designed to classify the input image into a specific class. For a well-trained DNN-based image classifier f , given an image x , one can get the output $f(x) = y_{cls}$, where $y_{cls} = y$, y_{cls} and y is the predicted class and ground truth of the input image, respectively, which are usually denoted as a scalar.

2) *Object detection task*: Object detection is another traditional task in computer vision, designed to locate the object in the image and simultaneously give the class of the located object. For a well-trained DNN-based object detector f , given an image x , one can get the output $f(x) = y_{obj}$, where y_{obj} contain three outputs including the bounding box, the confidence score, and category, where the bounding box contains two coordinates consists of four scalars, latter two terms are scalar value.

D. Form of perturbation

Unlike the attack designed to add perturbation to the whole image, physical adversarial attacks are devised to modify the

object region to mislead the target model, called instance-level attacks. The reason is that it is impossible to modify the background environment (e.g., sky) in the real world. In contrast, instance-level attacks concentrate on crafting the perturbation for the targeted object. Therefore, instance-level attacks are suitable for performing physical attacks. According to the form used to modify the target object, the perturbation can be categorized as the adversarial patch, adversarial camouflage texture, and optical attacks.

1) *Adversarial patch*: The adversarial patch is an image patch that can be stuck on the target object's surface. Thus, adversarial patch attacks have the advantage of easily performing physical attacks as the adversary only requires printing out the patch and then sticking/hanging it on the specific target object. In optimization, the adversarial patch is pasted on the target object, which is consistent with physical deployable. However, inconsistencies exist when the target object is not a plane, as it simply pastes on the plane target in the 2D image during optimization. Additionally, the adversarial patch merely works in the specific view. The above issues curb the usefulness of adversarial patches in the real world.

2) *Adversarial camouflage texture*: Adversarial camouflage texture attacks are designed to modify the appearance of the 3D object by the optimized adversarial texture, which can be wrapped/painted over the target object's surface, such as the pattern of clothes or the scrawl/painting of the vehicle. Thus, that perturbation is suitable for non-plane objects, making it remain consistent well with the deployment in physical attacks. There are two technology roadmaps to optimize the texture. One is to optimize a 2D image as the texture of the target object; The other is to optimize a 3D texture directly with the help of a physical renderer.

3) *Optical attacks*: Unlike adversarial patch or camouflage texture attacks, optical attacks are designed to modulate the light or laser to perform physical attacks. In physical attacks, the adversary emits the light/laser by the lighting device (e.g., projector and laser emitter) toward the target object to modify its appearance for attacking the target model. Thus, optical attacks are controllable and well stealthy. However, optical attacks are susceptible to environmental light, which curbs their utilization in practice.

E. Way of physical adversarial attack

According to whether the target object requires to be modified, the implementation way of physical attacks can be categorized into invasion attacks and non-invasion attacks.

1) *Invasion attacks*: Invasion attacks mean that the adversarial perturbation would modify the object itself. For instance, in attack facial recognition, the adversary wears an adversarial hat and glasses; In attack pedestrian detection, the adversary wears clothes or holds an adversarial patch plane; In attack vehicle detection, the adversary modifies the appearance of the vehicle by pasting the adversarial patch or painting the adversarial camouflage over the surface of the object to be attacked.

2) *Non-invasion attacks*: Non-invasion attacks do not require the adversary to modify the target object manually. In

TABLE I
TRANSFORMATION DISTRIBUTION REPORTED IN [45]–[48].

Transform	Parameters	Remark
Affine	$\mu = 0, \sigma = 0.1$	Perspective/Deformed Transforms
Rotation	$-15^\circ \sim 15^\circ$	Camera Simulation
Contrast	$0.5 \sim 1.5$	Camera Parameters
Scale	$0.25 \sim 1.25$	Distance/Resize
Brightness	$-0.25 \sim 0.25$	Illumination
Translation	$-0.04 \sim 0.04$	Pattern Location
Cropping	$-0.7 \sim 1.0$	Photograph/Occlude Simulation
Random Noise	$-0.15 \sim 0.15$	Noise

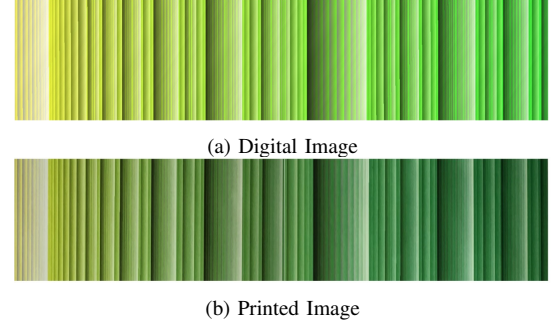


Fig. 2. Visualization discrepancy between the digital image (a) and its printed images (b). [50]

contrast, the adversary implements non-invasion attacks by projecting a shadow or emitting a laser toward the target object, which is more stealthy and dangerous. Optical attacks fall into this type.

F. Techniques for enhancing the robustness of physical attacks

1) *Expectation Over Transformation (EOT)*: EOT is a general framework for improving the adversarial robustness of physical attack on a given transformation distribution \mathcal{T} [49]. Essentially, EOT is a data augmentation technique for adversarial attacks, which takes potential transformation in the real world into account during the optimization, resulting in better robustness. Table I provides the widely used transformations reported in [45]–[48]. Specifically, rather than taking the norm of $x - x'$ to constrain the solution space, given a distance function $d(\cdot, \cdot)$, EOT instead aims to constrain the expected effective distance between the adversarial and original inputs under a transformation distribution, which expressed as

$$\delta = \mathbb{E}_{t \sim \mathcal{T}}[d(t(x'), t(x))]. \quad (2)$$

Note that, this survey categorizes the methods that used the transformation as EOT for simplicity.

2) *Non-Printability Score (NPS)*: One necessary way to perform physical attacks is to print the adversarial perturbation. Thus, the perturbation will inevitably have some distortion caused by the printer, resulting in attacks failing in some cases. For instance, Figure 2 illustrates the digital color and its printed result. To address this issue, non-printability score (NPS) loss [51] is devised as a metric to measure the color distance between optimized adversarial perturbation and the common printer. In general, the NPS loss can be represented as the following loss

$$L_{nps} = \sum_{p(i,j) \in x_{adv}} \min_{c_{print} \in C} |p(i,j) - c_{print}|, \quad (3)$$

where the $p(i,j)$ is a pixel at coordinate (i,j) in the adversarial example and c_{print} is a color in a set of printable colors C . Under the constraints of NPS loss, the optimized adversarial perturbation will gradually close to the predefined printable colors.

3) *Total variation norm (TV loss)* : Natural images have representative characteristics of smooth and consistent patches, where color is only gradually within patches [52]. Hence, finding smooth and consistent perturbations enhances the plausibility of physical attacks. In addition, due to sampling noise, extreme differences between adjacent pixels in the perturbation are unlikely to be accurately captured by cameras. Consequently, perturbations that are non-smooth may not be physically realizable [51]. To address the above issues, total variation (TV) [52] loss is presented to maintain the smoothness of perturbation. For a perturbation δ , TV loss is defined as

$$TV(\delta) = \sum_{i,j} ((\delta_{i,j} - \delta_{i+1,j})^2 + (\delta_{i,j} - \delta_{i,j+1})^2)^{\frac{1}{2}}, \quad (4)$$

where $\delta_{i,j}$ is a pixel in δ at coordinates (i,j) . $TV(\delta)$ is low when the values of adjacent pixels are close to each other (i.e., the perturbation is smooth) and vice versa [51]. Therefore, under the constraint of $TV(\delta)$ loss, the perturbation is gradually smooth and suitable for physical realizability.

4) *Digital-to-Physical (D2P)*: In some cases, EOT cannot cover all physical world transformations, such as the discrepancy between the digital image and the corresponding captured physical image caused by environmental factors. Thus, some researchers [53] proposed to utilize the digital image and the corresponding physical image pair (namely, D2P) to train the adversarial perturbation, reducing such discrepancy. D2P has been shown the effectiveness in improving the physical robustness of adversarial perturbation. Therefore, D2P can be regarded as an effective technique to boost the physical robustness of adversarial attacks.

G. Physical Testing environment

The common process of physical adversarial attacks is described as follows: first, optimize the adversarial perturbation in the digital world. Then, prepare the adversarial perturbation and paste/paint it over the target object, e.g., printing out the adversarial patch with the color printer and then hanging it on the object. Finally, place the adversarial perturbed object toward the deployed sensor device (e.g., RGB camera sensor) to perform attacks. Figure 3 provides an overview of the whole process of physical attacks. According to the relation between the adversarial object and the sensor device, the physical testing environment can be divided into stationary and dynamic.

1) *Stationary physical test*: The stationary physical adversarial test experiment is performed in a static physical environment, which means the adversary object and the sensor device maintain the static at the same time. For example, to attack the automatic checkout system, the adversarial sticks the adversarial patch to the surface of the commodity and place it under the sensor input of checkout systems [29], [54].

2) *Dynamic physical test*: The dynamic physical test is performed in a dynamic environment, which makes it more challenging. The reason is that more factors will impact perturbation as the changing environment. Thus, the dynamic physical test includes three different forms 1) the adversarial object is fixed while the sensor device is moving (e.g., drone surveillance); 2) the adversarial object moving while the sensor device is fixed (e.g., video surveillance); 3) both the adversarial object and the sensor device are moving simultaneously (e.g., automatic driving).

According to devised taxonomy scheme, we summarize the existing physical adversarial examples of image recognition and object detection task in Table II and Table III separately, and we provide the follow-up update in <https://github.com/winterwindwang/Physical-Adversarial-Attacks-Survey>. The organization of the following paper is that we review the physical adversarial attack against the image recognition tasks in Section IV and object detection task in Section V. In Section VI, we discuss challenges to be solved. Then we provide some promising research directions for constructing better physical adversarial examples. Finally, we make a conclusion in Section VII.

IV. PHYSICAL ADVERSARIAL ATTACK ON IMAGE RECOGNITION TASK

Advanced deep learning techniques have been increasingly deployed in daily life. For instance, facial recognition in automatic payment, image recognition techniques are employed in auto checkout machines in the shopping center, and road sign recognition in the computer-aid drive of the automated vehicle. Therefore, a line of literature is proposed to investigate the security of these systems. In this section, we will discuss the existing physical attacks on image recognition tasks from general image recognition, facial recognition, and road sign recognition.

A. General image recognition

The early investigation of physical adversarial attacks against image recognition mainly focuses on verifying the possibility of physical attacks by printing the adversarial image. Later, more realistic settings are explored, such as the utilization of adversarial patches [59] or adversarial viewpoints [61].

1) *Iterative Fast Gradient Sign Method (I-FGSM)*: Unlike exploring the adversarial examples in the digital world, Kurakin *et al.* [55] investigated the possibility of adversarial examples in the physical world. Specifically, the author optimized the adversarial examples by iterative updates along

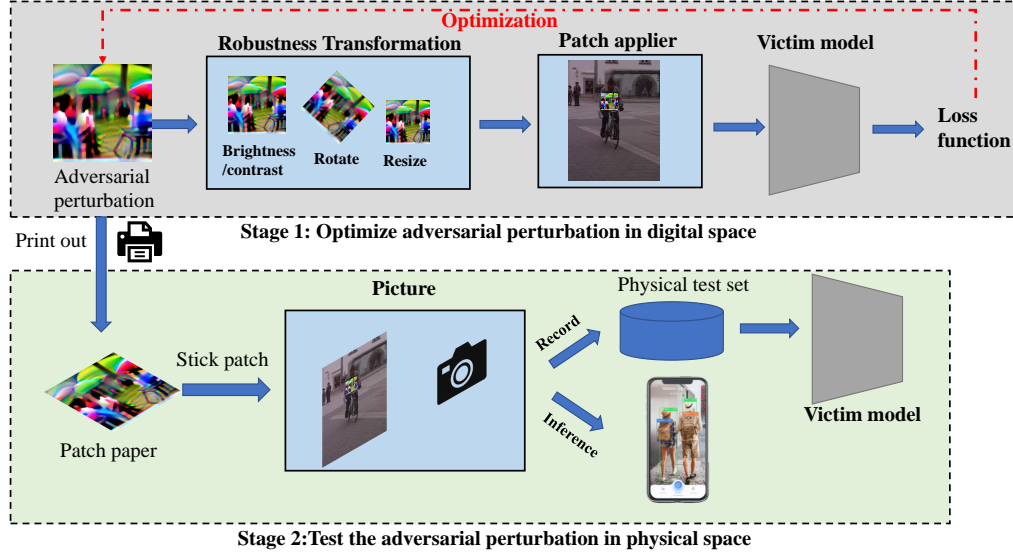


Fig. 3. Overview of the physical adversarial attack process.

the direction of the gradient ascent multiple times in small steps. The attack algorithm can be expressed as follows.

$$\begin{aligned} x_{adv}^0 &= x, \\ x_{adv}^{N+1} &= \text{Clip}_{x,\epsilon} \{x_{adv}^N + \alpha \text{sign}(\nabla_x J(x_{adv}^N, y))\} \end{aligned} \quad (5)$$

where α controls the iterative step, ϵ is the maximum allowable modification over the image, $\text{Clip}_{x,\epsilon}(\cdot)$ is a function to confine the discrepancy between adversarial examples and clean image in ϵ . In physical attacks, the author printed adversarial examples and used a phone to capture the photo of adversarial examples. Experiment results suggested that the printed adversarial examples can fool the image recognition model.

2) *EOT*: To construct robust adversarial examples for physical attacks, Athalye *et al.* [49] proposed a general framework to synthesize robust adversarial examples over a set of transformation distributions, which called Expectation Over Transformation (EOT). Specifically, they constructed the the following optimization problem

$$\begin{aligned} &\underset{x'}{\text{argmin}} \mathbb{E}_{t \sim \mathcal{T}} [\log \text{Pr}(y_t | t(x'))] \\ &- \lambda \| \text{LAB}(t(x')) - \text{LAB}(t(x)) \|_2, \end{aligned} \quad (6)$$

where the $\text{Pr}(y_t | t(x'))$ represents the probability of $t(x')$ be classified to y_t , which is used to guarantee the adversarial; $\text{LAB}(\cdot)$ is the color space convert function between RGB space to LAB space, which used to ensure the perceptual of adversarial perturbation. Note that, they develop an algorithm to optimize the texture of 3D objects in 3D cases scenario. In physical attacks, the author printed the 3D object and the adversarial texture with the printer (3D), then wrapped the adversarial texture over the 3D object. Evaluations were conducted on the captured image, and the results suggested that the multi-view captured images can fool the image recognition model.

3) *D2P*: Take further steps than [55], Jan *et al.* [53] analyzed the discrepancy between the digital image and the physical adversarial image, then proposed a method to modeling such difference. Specifically, the author first collected enormous digital-physical image pairs by printing digital images and retaking them. Then, the author treated the transformation between the digital and physical worlds as the image-to-image translation and adopted a Pix2Pix model [106] or a CycleGAN [107] to learn the translation mapping. Additionally, the EOT is adopted to boost the robustness of the adversarial perturbation on the simulated physical image (i.e., the generator's output). In physical attacks, the author printed out the adversarial examples and retook them every 15 degrees in the range of $[-60, 60]$. Experiment results suggest that their attack outperforms the EOT and remains valid under different visual angles. However, their attack is the full pixel attack, which is impractical in practice.

4) *ABBA*: Guo [56] proposed a novel motion attack, which exploits the blurring effect caused by object motion to fool the DNNs. Specifically, the author optimized the specific transform parameters for the object and background to create the blurring effect. The background is extracted by a binary mask generated with a saliency detection model. Moreover, the author used a spatial transformer network [108] to improve the robustness of adversarial examples. In physical attacks, the author captured the object image in the real world and generated the adversarial blur examples by the devised method. Then, the author moved the camera according to the optimized transformation parameters to take the blurred image. Experiment results show that the captured blurring image achieved a success rate of 85.3%.

5) *MetaAttack*: Feng *et al.* [57] observed that the previous D2P requires enormous amounts of manually collected data and proposed to utilize the meta-learning technique to solve the problem. Specifically, the author proposed to use GAN

TABLE II
PHYSICAL ADVERSARIAL ATTACKS AGAINST IMAGE RECOGNITION TASKS. WE LIST THEM BY TIME AND TASK, ALIGNING WITH THE PAPER'S DISCUSSION ORDER.

Method	Year-Venue	Adversarial's Knowledge	Threat Model	Adversarial Specificity	Robust Technique	Physical Test Type	Space	Remark	Code
I-FGSM [55]	2017-ICLR	White-box	Classification	Targeted/Nontargeted	-	Static	2D	Pixel-wise	✓
EOT [49]	2018-ICLR	White-box	Classification	Targeted	EOT	Static	2D	Pixel-wise	×
D2P [53]	2019-AAAI	White-box	Classification	Targeted	EOT,D2P	Static	2D	Pixel-wise	✓
ABBA [56]	2020-NeurIPS	White-box	Classification	Nontargeted	EOT	Static	2D	Pixel-wise	✓
MetaAttack [57]	2021-ICCV	White-box	Classification	Targeted	EOT	Static	2D	Pixel-wise	×
ISPAttack [58]	2021-CVPR	White-box	Classification	Targeted/Nontargeted	-	Static	2D	Pixel-wise	×
AdvPatch [59]	2017-NeurIPS	White-box	Classification	Targeted	EOT	Static	2D	Patch	✓
ACOsAttack [54]	2020-ECCV	White-box	Classification	Nontargeted	EOT	Static	2D	Patch	✓
ACOsAttack2 [29]	2021-TIP	White-box	Classification	Nontargeted	EOT	Static	2D	Patch	✓
TnTAttack [38]	2022-TIFS	White-box	Classification	Targeted/Nontargeted	-	Static	2D	Patch	×
Copy/PasteAttack [60]	2022-NeurIPS	White-box	Classification	Targeted	EOT,TV	Static	2D	Patch	✓
ViewFool [61]	2020-NeurIPS	White-box	Classification	Nontargeted	-	Static	3D	Position	✓
LightAttack [62]	2018-AAAI-S	Black-box	Classification	Targeted/Nontargeted	EOT	Static	2D/3D	Optical	×
ProjectorAttack [63]	2019-S&P	White-box	Classification	Targeted	-	Static	2D	Optical	×
OPAD [64]	2021-ICCV-W	White-box	Classification	Targeted/Nontargeted	EOT	Static	2D	Optical	×
LEDAttack [65]	2021-CVPR	White-box	Classification	Targeted/Nontargeted	EOT	Static	2D	Optical	✓
AdvLB [66]	2021-CVPR	Black-box	Classification	Nontargeted	-	Static	2D	Optical	✓
SLMAttack [67]	2021-arXiv	White-box	Classification	Nontargeted	-	Static	2D	Optical	×
SPAA [68]	2022-VR	White-box	Classification	Targeted/Nontargeted	D2P	Static	3D	Optical	✓
AdvEyeglass [51]	2016-CCS	White-box	FR	Targeted/Nontargeted	TV,NPS	Static	2D	Eyeglasses	×
AdvEyeglass2 [69]	2019-TOPS	White-box	FR	Targeted/Nontargeted	Color Adjust	Static	2D	Eyeglasses	✓
CLBAAttack [70]	2021-BIOSIG	White-box	FR	Targeted/Nontargeted	EOT	Static	2D	Eyeglasses	×
ReplayAttack [71]	2020-CVIU	White-box	FR	Targeted/Nontargeted	EOT,Position Adjust	Static	2D	Patch	×
ArcFaceAttack [72]	2019-SIBIRCON	White-box	FR	Targeted/Nontargeted	TV	Static	2D	Sticker	×
AdvHat [73]	2020-ICPR	White-box	FR	Nontargeted	TV,Bending	Static	2D	Sticker	×
TAP [74]	2021-CVPR	White-box	FR	Targeted/Nontargeted	EOT	Static	2D	Sticker	×
AdvSticker [39]	2022-TPAMI	Black-box	FR	Targeted/Nontargeted	Blending	Static	3D	Sticker	×
SOPP [75]	2022-TPAMI	Black-box	FR	Targeted/Nontargeted	-	Static	2D	Sticker	✓
AdvMask [76]	2022-ECMLPKDD	White-box	FR	Targeted/Nontargeted	Rendering	Static	3D	Mask	✓
LPA [77]	2020-CVPR-W	White-box	FR	Targeted/Nontargeted	Position/Color Adjust	Static	2D	Optical	×
RP_2 [46]	2018-CVPR	White-box	TSR	Targeted/Nontargeted	D2P	Static	3D	Patch	×
RogueSigns [78]	2018-arXiv	White-box	TSR	Targeted	EOT	Dynamic	2D	Pixel-wise	✓
PS_GAN [79]	2019-AAAI	White-box	TSR	Nontargeted	-	Static	2D	Patch	×
AdvCam [80]	2020-CVPR	White-box	TSR	Targeted/Nontargeted	EOT	Static	2D	Pixel-wise	✓
ShadowAttack [81]	2022-CVPR	Black-box	TSR	Nontargeted	EOT	Static	2D	Optical	✓
AdvPattern [82]	2019-CVPR	White-box	ReID	Targeted/Nontargeted	EOT,TV	Static	2D	Patch	✓
PhysGAN [83]	2020-CVPR	White-box	SteeringModel	Nontargeted	D2P	Dynamic	2D	Pixel-wise	×
LPRAttack [84]	2020-C&S	Black-box	LPR	Targeted	-	Static	2D	Patch	×

Venue: Venue with postfix “-S” and “-W” indicates the symposium and workshop. **C&S** : Computers & Security. **CVIU**: Computer Vision and Image Understanding.

Threat Model: **FR**: Face Recognition. **TSR**: Traffic Sign Recognition. **LPR**: License Plate Recognition.

- in **Robust Technique** indicates that there are no specific techniques to enhance physical robustness.

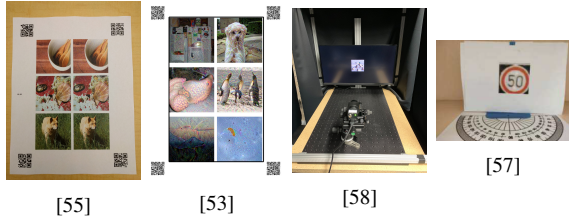


Fig. 4. Examples of physical adversarial example for general classification.

to generate adversarial examples. The generator’s parameters are trained via the meta-learning technique: for each task, the training set was split into the support set and query set, where the former is used to train the GAN, and the latter is used to validate it. The generator is trained on multi-tasks and fine-tuned on the new tasks in a few-shot learning manner. Moreover, EOT is adopted to enhance physical robustness. The physical experiments suggested that the captured adversarial image obtained a success rate of 95.2%.

6) *Attack Imaging pipelines*: Unlike modifying the pixel of the RGB images, Phan *et al.* [58] proposed to modify the RAW image that outputs from the camera device directly, which makes it robust to compression (i.e., JPEG). They demonstrated that perturbations devised for RAW images

remain physically aggressive when printed out and retaken by the camera.

7) *Adversarial patch (AdvPatch)*: Concurrent to [49], Brown *et al.* [59] first presented a general framework to construct the adversarial patch, which is robustness under a variety of transformations. Given that a small perturbation cannot deceive the adversarial defense techniques, the author discarded the constraint on the magnitude of the adversarial patches and proposed to use a large perturbation to attack defense techniques. Specifically, they replaced a partial pixel of the image with the optimized adversarial patch and defined the *patch application operator* $A(p, x, l, t)$ to implement the replacement. $A(\delta, x, l, t)$ means applies the transformation t to the patch δ , and then paste patch δ to the image x at location L . To construct the robust adversarial patch, they combine the EOT and propose the following optimization problem

$$\hat{\delta} = \underset{\delta}{\operatorname{argmin}} \mathbb{E}_{x \sim X, t \sim \mathcal{T}, l \sim L} [\log \Pr(y_t | A(\delta, x, l, t))] + \|\delta\|_{\infty}. \quad (7)$$

By solving the above problem, one can obtain the adversarial patch that could successfully mislead the DNN-based application to output the specific class y_t on the smartphone.

TABLE III

PHYSICAL ADVERSARIAL ATTACKS AGAINST OBJECT DETECTION TASKS. WE LIST THEM BY TIME AND TASK, ALIGNING WITH THE PAPER’S DISCUSSION ORDER.

Method	Year-Venue	Adversarial’s Knowledge	Threat Model	Adversarial Specificity	Robust Technique	Physical Test Type	Space	Remark	Code
ShapeShifter [45]	2018-ECMLPKDD	White-box	OD	Targeted/Nontargeted	EOT	Dynamic	2D	Pixel-wise	✓
RP2+ [50]	2018-USENIX-W	White-box	OD	Targeted/Nontargeted	TV,NPS,D2P	Static	2D	Patch	×
AdvPatch [47]	2019-CVPR-W	White-box	OD	Nontargeted	EOT,TV,NPS	Dynamic	2D	Patch	✓
NestedAE [85]	2019-CCS	White-box	OD	Targeted/Nontargeted	D2P, Physical Adjust	Dynamic	3D	Patch	×
DPatch2 [86]	2019-ICML	White-box	OD	Targeted/Nontargeted	EOT	Static	2D	Patch	×
LPAttack [87]	2020-AAAI	White-box	OD	Targeted	EOT,TV,NPS	Static	2D	Pixel-wise	×
TranslucentPatch [88]	2021-CVPR	White-box	OD	Targeted/Nontargeted	Affine,NPS	Static	2D	Patch	×
SwitchPatch [89]	2022-arXiv	White-box	OD	Targeted	TV	Static	2D	Patch	×
ScreenAttack [90]	2020-arXiv	White-box	OD	Targeted	TV	Static	2D	Patch	×
Invisible Cloak1 [91]	2018-UEMCON	White-box	OD	Nontargeted	EOT,TV	Static	3D	Wearable Patch	×
Adversarial T-Shirt [92]	2020-ECCV	White-box	OD	Targeted	EOT,TPS	Static	2D	Wearable Patch	×
Invisible Cloak2 [93]	2020-ECCV	White-box	OD	Nontargeted	TPS	Static	2D	Wearable Patch	✓
LAP [94]	2021-MM	White-box	OD	Nontargeted	TV,NPS	Static	2D	Wearable Patch	×
NaturalisticPatch [95]	2021-ICCV	White-box	OD	Nontargeted	TV	Static	2D	Wearable Patch	✓
AdvTexture [96]	2022-CVPR	White-box	OD	Nontargeted	EOT,TPS	Static	2D	Wearable Patch	✓
SLAP [97]	2021-USENIX Security	White-box	OD	Nontargeted	EOT,TV	Static	2D	Optical	✓
MeshAdv [98]	2021-CVPR	White-box	OD	Nontargeted	-	Static	3D	Shape	×
CAMOU [99]	2019-ICLR	White-box	OD	Nontargeted	EOT	Static	2D	Camouflage	×
ER [100]	2020-arXiv	Black-box	OD	Nontargeted	-	Static	3D	Camouflage	×
UPC [48]	2020-CVPR	White-box	OD	Targeted/Nontargeted	EOT	Static	3D	Camouflage	✓
DAS [30]	2021-CVPR	White-box	OD	Nontargeted	TV	Static	3D	Camouflage	✓
FCA [33]	2022-AAAI	White-box	OD	Nontargeted	TV	Static	3D	Camouflage	✓
CAC [34]	2022-IJCAI	White-box	OD	Targeted	EOT	Static	3D	Camouflage	×
DPA [35]	2022-CVPR	White-box	OD	Nontargeted	EOT	Static	3D	Camouflage	×
BulbAttack [31]	2021-AAAI	White-box	IR OD	Nontargeted	EOT,TV	Static	2D	Optical	×
QRAttack [32]	2022-CVPR	White-box	IR OD	Nontargeted	EOT	Static	2D	Patch	×
AerialAttack [101]	2022-WACV	White-box	ODAI	Targeted	EOT,TV,NPS	Dynamic	2D	Patch	✓
RWAE [102]	2022-WACV	White-box	SS	Nontargeted	EOT	Static	2D	Patch	✓
MDEAttack [103]	2022-ECCV	White-box	MDE	Nontargeted	EOT	Static	2D	Patch	×
PATAttack [104]	2019-ICCV	White-box	OT	Targeted/Nontargeted	EOT	Dynamic	2D	Patch	×
MTD [105]	2021-AAAI	White-box	OT	Targeted	EOT,TV	Dynamic	2D	Patch	×

OD: Object Detection. **SS:** Semantic Segmentation. **MDE:** Monocular Depth Estimation. **IR OD:** Infrared Object Detection. **ODAI:** Object deTecton in Aerial Images. **OT:** Object Tracking. Venue with postfix “-W” indicates the workshop.

- in **Robust Technique** indicates that there are no specific techniques to enhance physical robustness.

However, lacking constraint on perturbation results in the odd appearance of the adversarial patch.

8) *ACOsAttack*: The previous physical attacks failed to explore the DNN-based application in real life, Liu *et al.* [29], [54] proposed optimizing a universal adversarial patch to attack the real deployed automatic check-out system (ACOs). Specifically, the author exploits models’ perceptual and semantic biases to optimize the adversarial patch. Regarding the perceptual bias, the author used hard examples which convey strong model uncertainties and extracted the textural patch prior from them in terms of the style similarities. To alleviate the heavy dependency on large-scale training data, the author exploited the semantic bias by collecting many prototypes with respect to the different classes, then trained the universal adversarial patch on the prototype dataset. Moreover, the author also adopted the EOT to improve the robustness of the adversarial patch. In physical attacks, the author printed the adversarial patch and stuck them on the commodities, then captured it from different environmental conditions (i.e., angles $\{-30^\circ, -15^\circ, 0^\circ, 15^\circ, 30^\circ\}$ and distances $\{0.3, 0.5, 0.7, 1\}$)(meter). Experiment results suggested that the captured images with the adversarial patch easily deceive the system. Additionally, their attack could degrade the recognition accuracy of the prevalent E-commerce platforms (i.e., JD and Taobao) on the test set by 43.75% and 40%.

9) *TnTAttack*: Recently, Bao [38] *et al.* pointed out the existing physical adversarial patches are visually conspicuous. To address the issue, the author proposed to exploit a generator

to construct naturalistic adversarial patches. Unlike crafting full-pixel adversarial examples with GAN [109], the author first train a generator to map the latent variable z (i.e., random noise) to the realistic image patch, which will be embedded in the image. In the second stage, the author fixed the generator’s parameters, then used the gradient-based optimization method with the guide of adversarial loss to seek the optimal latent variable z , which generates the visual naturally adversarial patch. Their approach is based on the fact that the trained generator could map the randomly sampled latent variable z to a naturalistic image, in which one latent space can be mapped to the naturalistic adversarial patch. In such a way, the author significantly reduced the optimization variable (only 100-dimension latent variables z). In physical attacks, the author printed the patch image and stuck it on the front of clothes, then captured a 1-minute video of the person who wore the clothes with the adversarial patch. Experiment results suggested that over 90% of captured images in frames can fool the target network.

10) *Copy/Paste Attack*: Inspired by the ringlet butterfly’s predators being stunned by adversarial “eyesspots” on its wings, Casper [60] speculate that the DNNs are fooled by interpretable features in the real world. To this end, the author proposed to develop adversarial perturbation that can reveal the weakness of the victim network. Specifically, the author used GAN to create the patch, which is pasted on the target image that is classified as the specific target class by the target model. Additionally, EOT is adopted to improve the

adversarial patch’s robustness, and TV loss is adopted to discourage high-frequency patterns. In physical attacks, the author printed the adversarial patch and pasted it on the object. Evaluation results on the recaptured image verify the effectiveness of their method in the real scenario.

11) *ViewFool*: Unlike generating the adversarial perturbation by modifying the pixel of images, [61] suggested the existence of adversarial viewpoints in the real world, which means that the image taken at a specific view is sufficient to fool the model. To search such viewpoints, the author treats the coordinate and orientation (i.e., yaw, roll, pitch) of the camera in the world axis as the optimization variables and exploits the NeRF to render the object with the searched coordinate and orientation. In physical attacks, the author takes pictures from adversarial viewpoints and evaluates the attack performance. Experiment results suggest that DNN models are vulnerable to adversarial viewpoints.

12) *Optical attacks*: Unlike adversarial patch attacks, optical attacks are more stealthy and controllable as the attacker is not required to modify the target object. One representative characteristic of optical attacks involves the projector-camera model, a process for improving the robustness of physical attacks. It refers to projecting the adversarial perturbation into the real world by the projector and recapturing it by the camera for evaluation. For this reason, Nichols *et al.* [62] first collected hundreds of real projected and captured image pairs as the training dataset, then they got inspiration from the one-pixel attack and adopted the differential evolution (DE) to optimize one pixel as the projection point in the low-resolution image (e.g., 32×32). In physical attacks, the author projected the light over the specific area of the object and recaptured it. Experiment results demonstrate the effectiveness of light attacks.

In contrast to [62], Man *et al.* [63] performed physical attacks by projecting a light source over the whole image. Specifically, to ensure the emitted light can impact the image to fool the classifier, the author treated the color distribution (the means and the standard deviations of the Gaussian distribution) of light as an optimization problem. In physical attacks, the author modulated the projector’s color (the value of RGB) to emit the light to the displayed image, then took the photo for testing. Cased studies verify the effectiveness of physical attacks. Gnanasambandam *et al.* [64] considered the projector factor and devised a transform function consisting of a matrix and an offset to mimic the process of converting images to the physical scene, where the matrix is used to transfer the image to projector space; and the offset is used to counteract the background illumination. In optimization, the transform function is performed first, followed by the gradient-based algorithm (i.e., PGD [12]). Concurrent to [64], Kim *et al.* [67] modulated the phase of the light in the Fourier domain using a spatial light modulator (SLM) to yield the adversarial attack, where the modulator’s parameters are optimized with gradient-based algorithms. Sayles *et al.* [65] modulated a light signal to illuminate the object then its surface displays striping patterns, which could mislead the classifier to make a mistake in physical attacks. Duan *et al.* [66] modulated a laser beam to perform adversarial attacks, where the laser’s wavelength,

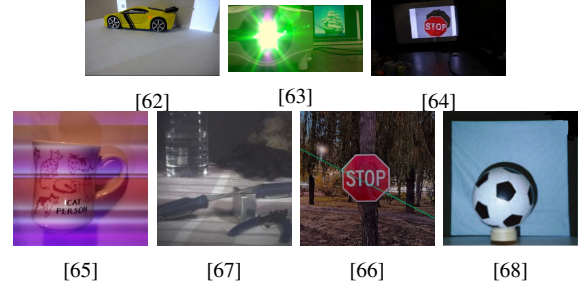


Fig. 5. Examples of optical attacks.

layout, width, and intensity are optimized by random search.

Recently, Huang *et al.* [68] proposed a stealthy projector-based adversarial attack (SPAA) method, which formulated the physical projector attack as an end-to-end differentiable process. Specifically, the author devised a PCNet to approximate the project-and-capture process, which could optimize the adversarial perturbation on the projected-captured image pairs under the guidance of adversarial loss and stealthiness loss. In physical attacks, the author projected the adversarial perturbation on the target object 1.5 meters away from the projector and recaptured it for evaluation. Experiment results demonstrated that the stealthy adversarial perturbation generated by SPAA could deceive the DNN significantly.

Figure 5 illustrates examples of various optical attack methods. However, despite its stealthiness and controllability, optical attacks are constrained by many factors, such as the object’s surface material, the color’s saturation, and the scene’s light intensity. However, despite its stealthiness and controllability, optical attacks are constrained by many factors, such as the object’s surface material, the color’s saturation, and the scene’s light intensity.

13) *AdvPattern*: In contrast to the image recognition task, Wang *et al.* [82] first attempted to implement the physical adversarial attack against the person re-identification (re-ID). To improve the physical robustness of the adversarial pattern, they devise a degradation function (i.e., a kind of data augmentation technique) that randomly changes the brightness or blurs the adversary’s images from the augmented generated set, which is constructed by a multi-position sampling strategy. Such a strategy is essentially used to boost the performance of an attack under a multi-camera view. For the physical adversarial experiment, the author printed out the adversarial pattern and attached it to the adversary’s clothes, and applied the physical attack under the condition of distance ($4 \sim 10$ meter) and angle ($12^\circ \sim 47^\circ$).

B. Facial Recognition

Facial recognition is a technique to match a human face from a digital image or video frame against a database of faces. In general, the first step of facial recognition is to extract the face area of the input image and feed it into the facial recognition system to predict/match the concrete person. Thus, the adversarial attack against facial recognition can be categorized into dodging and impersonation attacks; the former refers to the adversary seeking the adversarial perturbation to mislead the face to the specific face, while

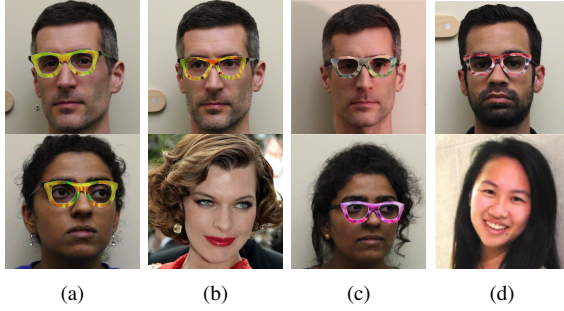


Fig. 6. Examples of adversarial glasses for dodging and impersonation attacks of [51] (a,b) and [69] (c,d).

the latter refers to the attacked face that can be misidentified as other face except the original one. Actually, the dodging and impersonation attack is analogous to the untargeted and targeted attacks, respectively. Specifically, physical attacks against the facial recognition system to output the incorrect person (impersonation attack) or undetected result (dodging attack) by modifying the accessorize of the face, e.g., eyeglasses frame [51], [69], hat [73], sticker [39], or even makeup [110].

1) *Eyeglass attack*: Sharif *et al.* [51] first investigated the physical adversarial attack against face recognition models. To attack the face recognition model, they taken the facial accessory (i.e., eyeglasses) as the perturbation carrier. The robustness of the single perturbation is enhanced by training it on a set of images, making it remain works under different imaging conditions. Additionally, the TV loss [52] is adopted to improve the smoothness of perturbation and designed the NPS loss to ensure the printability of perturbation. Finally, the author optimizes the perturbation by constructing the following optimization problem

$$\begin{aligned} \operatorname{argmin}_{\delta} & \left(\sum_{x \in X} \operatorname{softmaxloss}(x + \delta, y_t) \right) \\ & + \kappa_1 \cdot TV(\delta) + \kappa_2 \cdot NPS(\delta), \end{aligned} \quad (8)$$

where *softmaxloss* is the adversarial loss for the face recognition system, κ_1 and κ_2 balance the objectives. To conduct the physical experiment, the author printed and cropped out the adversarial eyeglass frame and stuck it on the actual pair of eyeglasses. Then, the author asked the trial participant to wear eyeglasses and stand at a fixed camera distance in the indoor environment and then collected 30-50 images for each participant. Experiment results suggested that their adversarial eyeglass frame easily deceives face recognition.

Although the eyeglasses frame generated by [51] deceive facial recognition to some extent, Sharif *et al.* [69] argued that the appearance of the eyeglasses frame is conspicuous. To craft an inconspicuous eyeglass frame, the author proposed to use a generative model to craft the adversarial glasses frame with a natural pattern. Specifically, the author first collected enormous images of real glasses frames as the training set; Then trained an adversarial generative network (AGN) with the following loss function, i.e., Equation 9 and 10 for the untargeted and targeted attack, respectively.

$$\begin{aligned} \mathcal{L}_G^{\text{untargeted}} &= \sum_{z \in Z} \lg(1 - D(G(z))) \\ &- \kappa \left(\sum_{i \neq x} F_{y_i}(x + G(z)) - F_{y_t}(x + G(z)) \right), \end{aligned} \quad (9)$$

$$\begin{aligned} \mathcal{L}_G^{\text{targeted}} &= \sum_{z \in Z} \lg(1 - D(G(z))) \\ &- \kappa (F_{y_t}(x + G(z)) - \sum_{i \neq t} F_{y_i}(x + G(z))), \end{aligned} \quad (10)$$

where the z is sampling from a distribution Z , $D(\cdot)$ and $G(\cdot)$ are the output of discriminator and generator, respectively. F_{y_t} and F_{y_i} are the network's softmax output of the ground-truth label y_t and another label y_i . $\lg(\cdot)$ is the logarithmic function and κ is the weight to balance the loss function. By minimizing the loss function, the generator learns to craft realistic glasses frames with adversarial. To further enhance the robustness of the adversarial glasses in physical attacks, the author introduce the following three methods. The first one is to utilize multiple images of the attacker to improve the robustness of adversarial glasses under different conditions. The second is to collect various pose images to make the attacks robust to pose changing. The third is to use the Polynomial Texture Maps approach [111] to confine the RGB value of eyeglass under baseline luminance to values under a specific luminance, making the attacks robust to varying illumination conditions. In physical attacks, the author printed out the eyeglasses frame and adversarial pattern, stuck them over the eyeglasses frame, and then recaptured images for evaluation. Experiment results show that their method outperforms [51] by the improvement of 45% under different physical conditions (i.e., head pose covered 13.01° pitch, 17.11° of yaw, 4.42° of roll). Figure 6 illustrates the printed adversarial eyeglasses generated by [51] and [69].

Later, Zhang *et al.* [71] demonstrated that the face authentication system equipped with the DNN-based spoof detection module is still vulnerable to the adversarial perturbation. They got inspiration from EOT [49] and train the perturbation over a serial of transformations (i.e., affine, perspective, brightness, gaussian blurring, and hue and saturation). In performing physical attacks, The author displayed the face image with adversarial perturbation on the screen and then captured it by the cellphone under different views (angles in $-20^\circ \sim 20^\circ$, distances in 10 to 50 cm). Experiment results suggested that the target system is fragile to the adversarial face image.

Recently, Singh *et al.* [70] leveraged the concept of curriculum learning to promote the robustness of attack to changing brightness against the facial recognition model. In optimization, the author constantly changes the brightness of face images stuck with adversarial eyeglasses, which makes their attack robust to brightness changes. Physical attacks verify the effectiveness of the attack against the brightness change.

2) *Sticker*: Unlike treating the eyeglasses as the perturbation carrier, Pautov *et al.* [72] proposed a simple but effective method to craft the adversarial sticker to deceive face recognition. To apply the adversarial sticker over the facial area, the author applied the projective transformation over the

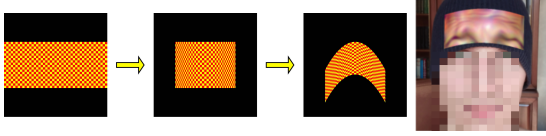


Fig. 7. Bend and rotation over the rectangle [73]. The length of the rectangle do not change.

adversarial sticker, then stuck the sticker on the nose or eye of the adversary. To optimize the sticker, the author treats the cosine similarity between the image embedded with the patch and the original clean image as adversarial loss, which is expressed as follows.

$$\mathcal{L}(X, \delta) = \mathbb{E}_{t \in \mathcal{T}, x \in X} [\cos(e_{x_t}, e_{x_{adv}})], \quad (11)$$

where e_{x_t} and $e_{x'}$ are the embedding corresponding to the desired person x_t and the photo x_{adv} of the attacker with the applied patch. In addition, TV loss is adopted to constrain the visual effect of the adversarial sticker. To avoid the color discrepancy between the physical and the digital perturbation, the author chooses to optimize the sticker on a grayscale. They conduct the physical attack by printing out various shapes (i.e., eyeglasses and stickers) of stickers and stick on a specific area of the face. Experiment results show that their sticker can dramatically deteriorate FaceID models.

Komkov *et al.* [73] devised the adversarial sticker with the rectangle shape, which is stuck on the hat to attack the FaceID model. To optimize the adversarial sticker for the hat, the author first applied the bends and rotation (see Figure 7) transformation over the sticker to approximate the actual sticker process, which is realized by performing a differentiable formula on the pixel. The adversarial loss (i.e., cosine similarity distance) and TV loss are adopted to optimize the adversarial sticker. In physical attacks, the author stuck the adversarial sticker on the forehead area of the hat. Experiment results show that the person wearing the generated adversarial sticker easily bypasses the Face ID system (e.g., ArcFace).

Concurrent to [73], Xiao *et al.* [74] proposed to improve the transferability of the adversarial patch for face recognition systems. The author analyzes the drawback of existing transferability methods: sensitive to the initialization (e.g., MIM [13]) and exhibits severe overfitting to the target model when the magnitude of perturbation is substantial. To address these issues, the author regularizes the adversarial patch in a low-dimensional manifold represented by a generative model regularization. In optimization, the adversarial patch is bent and pasted on the eye area of the face. The author conducts the physical attack by printing and photographing the adversarial patch stuck in the human eye and achieves successful attacks.

Unlike optimizing the pattern or color of adversarial perturbation to perform attacks, Wei *et al.* [39] claimed that the natural image patch is sufficient to attack facial recognition models. Specifically, the author proposes a general framework for searching the most sensitive area of the model that is susceptible to the sticker. The author first locates the most vulnerable area by traversing the face image with a patch image, which accelerates the search speed. In optimization, the author

used the bend and rotation transformation in the 3D space to transform the adversarial patch to mimic the deformation of the sticker on the real face. In physical attacks, the author sticks the adversarial patch on the attacker's face according to the searched coordinate. Experiment results demonstrated that the natural image patch stick at the searched areas is sufficient to degrade the performance of DNN in digital and physical conditions.

Recently, Wei *et al.* [75] found that the position and the pattern of adversarial patches are equally significant to a successful attack. Thus, the author optimizes the positions and simultaneously perturbation against the face recognition model. Specifically, the author used a UNet architecture to generate the position and the attack step of the existing gradient-based algorithm (e.g., I-FGSM [55]) to reduce the optimization variables. In optimization, the author adopted the reinforcement learning framework to model the above problem, where the agent is the UNet, the policy is the sampling strategy in the agent, the action is specific optimization variables obtained by policy, and the rewards are generated by querying the ensemble model with the constructed adversarial examples. In physical attacks, the author printed the adversarial patch with photo paper as it can reduce the color discrepancy as much as possible. Experiment results on their method achieved an average success rate of 66.18% on captured images.

In the prevalence of the COVID-19 pandemic, wearing masks has become common sense. Zolfi *et al.* [76] got inspiration from this and generated a mask-like universal adversarial patch, which makes the attack more stealthy. The adversary who wears the crafted adversarial mask can bypass the face recognition systems in some scenarios, e.g., airport. Specifically, the author proposed a mask projection method to convert the faces and masks into UV space to mimic actual wearing. The mask image is optimized by minimizing the cosine similarity loss and TV loss to ensure adversarial and smoothness. In addition, geometric transformations and color-based augmentations are adopted to improve the robustness of the mask. To perform physical attacks, the author makes the mask with two different materials regular paper and white fabric mask. The author recruited a group of 15 male and 15 female participants to wear the different devised masks, and the experiment result demonstrated that the model's performance declined significantly (i.e., from 74.83% to 5.72%, 4.61% for paper and fabric mask) on the face wore the adversarial mask.

3) *Light Projection Attack (LPA)*: Unlike the adversarial perturbation patch approaches, Nguyen *et al.* [77] exploited the adversarial light projection to attack the face recognition systems. The critical technique of the light project attack is calibrating the adversarial region and color between the projector and digital images. To address the issue, the author proposed two calibration approaches (i.e., manual assign and automatic obtain with a landmark detection) to constrain the adversarial area to calibrate the position. To calibrate the color between the digital adversarial pattern and the physical version of adversarial light emitted by the projector, the author presented a color transformation function γ (Equation 12) to implement the conversion between the camera (C) and



Fig. 8. Examples of adversarial stickers or light projections.

projector (\mathcal{G}).

$$\begin{aligned}
 C(\hat{x}_{adv} + \mathcal{G}(\gamma(h(x)))) &= x + h(x) \\
 \iff C(\hat{x}_{adv}) + C(\mathcal{G}(\gamma(h(x)))) &= x + h(x) \\
 \iff C(\mathcal{G}(\gamma(h(x)))) &= h(x) \\
 \iff \gamma &= (C \odot \mathcal{G})^{-1},
 \end{aligned} \tag{12}$$

where \hat{x}_{adv} is the physical adversarial example, $h(x)$ represents the algorithm to search adversarial perturbation. Additionally, the author pointed out that γ in Lab color space can better approximate the physical domain RGB color space. In physical attacks, the author projects the adversarial light on the adversary's face to attack the facial recognition model.

To sum up, the main attack pipeline against facial recognition can be briefly described as follows. First, apply the adversarial perturbation precisely over the face area using bend and rotation or 2D/3D conversion via rendered. Meanwhile, a set of transformations or data augmentation are utilized to improve the robustness. Finally, the cosine similarity-based adversarial loss [70], [72], [73], [76], [77] and TV loss or NPS loss to ensure the physical deployable. Figure 8 display the examples generated by different methods.

C. Traffic sign recognition

Traffic sign recognition is one of the widely used applications of the DNN model, which can be deployed in various scenarios, such as road sign recognition in automatic driving or license plate recognition in auto-checkout parking lots. Therefore, a line of work has been proposed to explore the security risk of these models.

1) *RP₂*: Eykholt *et al.* [46] first demonstrated that the road sign recognition model is vulnerable to physical adversarial attack. The author proposed to optimize multiple white-black blocks with rectangle shapes. Specifically, the author first collected considerable physical traffic sign images as the training set to improve the robustness of adversarial patches to various physical environmental conditions. Moreover, to eliminate the color discrepancy between the digital adversarial patch and the printed physical adversarial patch, they adopt the NPS loss to constrain the color of the adversarial patches. Finally, the author formulated the optimization of such physical deployable adversarial patches as the following optimization formal.

$$\begin{aligned}
 &\operatorname{argmin}_{\delta} \lambda \|M_x \cdot \delta\|_p + NPS \\
 &\mathbb{E}_{x_i \sim X^V} J(f(x_i + T_i(M_x \cdot \delta)), y),
 \end{aligned} \tag{13}$$

where the M_x is the binary mask of the location patches, and X^V is the training dataset consisting of digital and physical examples. In physical attacks, the author performs the experiments under various camera distances (i.e., 1.5, 3, and 12 meters) and angles (i.e., $0^\circ \sim 15^\circ$) on the adversarial patch. Additionally, they also conduct dynamic physical attacks by recording the video while driving the car toward the adversarial traffic sign. Experiment results suggested that their method can dramatically deceive the stop sign recognition model. Additionally, the author empirically found that 1) adversarial performance is easily impacted by the location of the mask; 2) the mask optimized by L_1 regularization show more sparse that represents the most vulnerable of the model, while the L_2 result in successful attacks at an earlier iterative step.

Concurrent to [46], Sitawarin *et al.* [78] proposed a general attack pipeline, which can generate the adversarial logo, traffic sign, and custom adversarial sign. In optimization, the author used a circle mask to ensure perturbation is added to the target area (e.g., traffic sign). In addition, a set of transformations is used to ensure robustness. Finally, the adversarial perturbation is optimized by minimizing the C&W adversarial loss [14]. To perform dynamic physical attacks, the author drove a car and recorded the video to capture the adversarial sign from far (80 feet away) to near. Experiment results showed their attack could achieve a 95.74% of attack success rate.

2) *PS_GAN*: Unlike the optimization-based attacks, Liu *et al.* [79] proposed to utilize the generative model to construct inconspicuous adversarial patches. Specifically, the author exploited the attention map extracted by the Grad-CAM [112] to guide the paste location of adversarial patches for better attack performance. Meanwhile, they minimized the discrepancy between the adversarial patch and the seed patch for better visual fidelity. Finally, they adopt GAN loss, adversarial loss, and the L_2 -norm loss that is calculated by the seed patch and the output of the generator to optimize the perturbation. In physical attacks, the author printed the adversarial patch and stuck it on the traffic sign (i.e., “Speed Limit 20”) in the street with varying angles (e.g., $\{0^\circ, 15^\circ, 30^\circ, -15^\circ, -30^\circ\}$) and distances (e.g., $\{1, 3, 5\}$ m). Experiment results suggested that most of the captured traffic sign images pasted with adversarial patches are misclassified by the model (from 86.7% to 17.2%).

3) *AdvCam*: Take further step than [79], Duan *et al.* [80] proposed a novel approach to camouflage the adversarial perturbation (i.e., *AdvCam*) into a natural style that appears legitimate to human observers. Specifically, they exploited the style transfer technique [113] to hide the large magnitude perturbations into customized styles, which makes attacks more stealthy. They adopt the following adversarial loss to maintain the aggressive

$$\mathcal{L}_{adv} = \begin{cases} \log(p_{y_{adv}}(x_{adv})), & \text{for targeted attack} \\ -\log(p_y(x_{adv})), & \text{for untargeted attack,} \end{cases} \tag{14}$$

where $p_{y_{adv}}(\cdot)$ is the probability output (softmax on logits) of the target model f with respect to class y_{adv} . The style loss and content loss were adopted to ensure style transfer and the TV loss is introduced to reduce the variations between adjacent pixels. Additionally, the author utilized various physical conditions (i.e., rotation, scale size, and lighting change) to boost the robustness of adversarial patterns in the real world. Moreover, the author experimentally demonstrated that the location and shape of the adversarial pattern had limited influence on the attack performance, e.g., the attack was valid even though the adversarial patch was far from the object. In physical attacks, the author prints the adversarial pattern on paper and then photos it at various angles and distances. Experiment results demonstrate the effectiveness of their approaches in physical attacks. However, although the generated adversarial examples with well stealthy, using the generated whole adversarial object (i.e., stop sign) to apply an attack is impractical in the real world.

4) *PhysGAN*: In general, simulating real physical transformations is impossible in the digital world. Unlike adopting EOT to improve the physical robustness of adversarial patches, Kong *et al.* [83] proposed a novel method to learn physical transformation from videos recorded in the real world by using a generative model (i.e., PhysGAN), which is then used to optimize the physical robust adversarial patch. Specifically, the author placed the adversarial poster on the target object of the video frame and fed it into a video feature extractor. The extracted features are simultaneously fed into the generator and the final classification head to calculate the loss. The author maximizes the distance between the clean and adversarial video in the classification output to ensure the adversarial of generated posters. Combined with the GAN's loss, the trained adversarial poster preserves stealthiness and can deceive the target model. In physical attacks, the author printed the adversarial poster and placed it on the side of the road, then recorded the video when driving past the adversarial poster. Experiment results show that the steer angle classification model is fragile to the physical printed adversarial poster.

5) *ShadowAttack*: Recently, Zhong *et al.* [81] argued that the pattern of perturbations generated by prior approaches is conspicuous and attention-grabbed for human observers. To this end, the author proposed to utilize the natural phenomenon (i.e., shadow) to perform physical attacks. Specifically, the author considers the shadow location and value to create the shadow. For shadow location, the author found an appropriate polygon determined by a set of vertices. Regarding the shadow value, the author uses the LAB color space rather than RGB to search for the optimal illumination component. Finally, the author finds the best shadow by exploiting the particle swarm optimization (PSO) strategy. Additionally, EOT was adopted to improve the robustness of the shadow attacks. In physical attacks, according to the optimized digital shadow, the author used a triangle board to create a shadow over the traffic sign. Experiment results suggested that the shadow attack could achieve the fooling rate of 95% in real-world scenarios.

Additionally, the license plate recognition (LPR) model has been demonstrated to be vulnerable to physical adversarial



Fig. 9. Examples of adversarial examples against traffic sign recognition.

attacks [84]. Rather than optimize the perturbation over the whole image pixel, Qian *et al.* [84] proposed to optimize the best position where to paste the adversarial patch. Specifically, the author first cut out characters of the plate and selected the victim character. Then the position to be pasted with the rectangle black block is optimized by the genetic algorithm. The author reveals that different license plate characters show different attack sensitivity. To perform physical attacks, the author first collects the car plate from the real world, then optimize the optimal position for attack. After that, the author pastes the black sticker on the real car plate at the optimized location and captures the image for evaluation. Experiment results show the vulnerability of the LPR model to physical adversarial attacks.

In summary, the examples of various physical attack against the traffic sign recognition model is provided in Figure 9.

V. PHYSICAL ADVERSARIAL ATTACK ON OBJECT DETECTION TASK

Object detection is a technique to locate and classify the object in the image, which is widely applied in video surveillance and automatic driving, where the target object is the vehicle, pedestrian, traffic sign, and so on. Existing object detectors can be divided into single-stage detectors and two-stage detectors. Single-stage detectors output the detection results directly, and the typically single-stage detectors include the YOLO series [44], [114], SSD [115], RetinaNet [116], and so on. By contrast, the two-stage detector first extracts the feature with respect to input via a backbone, then performs classification and regression over the feature to obtain the categories and bounding boxes. The typically two-stage detector includes Faster RCNN [117], Master RCNN [118], and so on. Nonetheless, both single-stage and two-stage object detectors have three outputs: bounding boxes, objectness, and category. Bounding boxes locate the possible object in the image, where objectness gives the confidence that the located area contains the object, and category give the classification results.

Performing the adversarial attack against object detection at least requires modifying one of three outputs, making it more challenges than attacking the image recognition tasks. The main way to perform a physical adversarial attack against object detection is to modify the attributes (e.g., appearance) of the object, including adversarial patch, adversarial camouflage, and other novel approaches (e.g., emitting the laser toward the object). Although the pixel-wise adversarial examples can also realize physical adversarial attacks by printing the image with adversarial perturbation, we ignore them because it is unrealistic for the adversary to modify the whole environment in practice.

A. Patch-based physical adversarial attack

Patch-based physical attacks mainly focus on generating the adversarial patch for the plane object. The most remarkable advantage is that it is easily deployable in physical attacks as the adversary can perform attacks by only printing it out and hanging it. Such a characteristic makes it a suitable carrier for perturbation in physical attacks.

1) *ShapeShifter*: Chen *et al.* [45] first demonstrated that the EOT could be applied to improve the robustness of adversarial patches in attacking two-stage object detectors (i.e., Faster RCNN [117]). The optimization based on C&W attack [14] is formulated as follows.

$$\begin{aligned} \operatorname{argmin}_{x_{adv} \in \mathbb{R}^{h \times w \times 3}} \mathbb{E}_{x \sim X, t \sim \mathcal{T}} \left[\frac{1}{m} \sum_{r_i \in \operatorname{rpn}(M_t(x_{adv}))} L_{f_i}(M_t(x_{adv}), y) \right] \\ + c \cdot \|\tanh(x_{adv}) - x_o\|_2^2, \end{aligned} \quad (15)$$

where $M_t(x_{adv}) = (M_t(x, \tanh(x_{adv}))$ is an operation that transforms an object $\tanh(x_{adv})$ using t and then paste it into the background image x with a binary mask; rpn represent the region proposal represented extracted by the first stage of Faster RCNN; the $L_{f_i}(M_t(x_{adv}), y)$ is the loss function of classification in the i -th region proposal; the last term is a regularization term that is used to balance the attack strength and the quality of the adversarial patch. In physical attacks, the author conducted extensive static and dynamic attacks under multi-view conditions. The experiment demonstrated the vulnerability of the object detector and the feasibility of the physical adversarial attack.

2) *DPATCH*: Inspired by the adversarial patch in image recognition tasks [59], Liu *et al.* [119] extend adversarial patch attack to object detector by simply attack the classification output of the detector. Although they demonstrated that the adversarial patch could successfully implement the targeted attack and non-target attack on to object detector, the validity of the physical adversarial attack is not verified.

3) *RP2+*: Following up the physical adversarial against image recognition model [46], Eykholt *et al.* [50] extended the RP2 algorithm to attack object detector. Specifically, they modify the adversarial loss for adapting to attack object detector under two strategies creation and disappearance attack. According to the observation that the detector is more tends to focus more on contextual areas for prediction, they take the object's position and size into account to constrain the adversarial patch, which is realized by performing rotation (in the Z plane) and position (in the X-Y plane). Additionally, they find the L_∞ lead to a very pixelated perturbation that hurts the attack performance, and then they adopt the total variation norm (TV loss [52]) instead of L_∞ to address this issue. The final optimization objective is expressed as follows.

$$\begin{aligned} \operatorname{argmin}_{\delta} \lambda \cdot TV(M_x \cdot \delta) + NPS \\ + \mathbb{E}_{x_i \sim X^v} J(f(x_i + T_i(M_x \cdot \delta)), y), \end{aligned} \quad (16)$$

where $J(\cdot, y)$ is the adversarial loss function devised for the object detector, which considers the classification output. In physical attacks under indoor and outdoor conditions, the

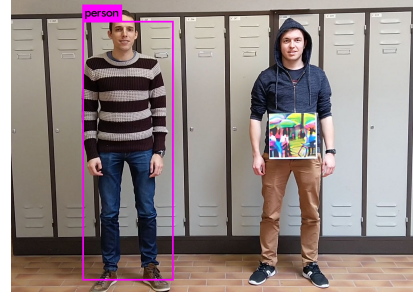


Fig. 10. Visualization of adversarial patch hiding the person under the surveillance camera. [47]

author captured the video of the adversarial object beginning away from 9 meters for the disappearance attack. By contrast, in the creation attack setting, they placed the adversarial patch on the wall or cupboard and captured the video from toward the adversarial object, away from 3 meters. The experiment result shows that the adversarial patch can mislead the YOLOv2 in most cases, demonstrating its fragility in practice. In addition, the experiment suggests that the indoor attack performs well than the outdoor attack, which can be attributed to the complex environment in the outdoor conditions.

The previous works [46], [59] were concentrated on the no intra-class variety (e.g., stop sign). To this end, Thys *et al.* [47] proposed to generate adversarial patches for intra-class variety (i.e., persons). They aim to hide the person who holds the printed adversarial patch cardboard plate and towards the device with the object detector application. In optimization, the author designed an algorithm to place the adversarial patch in the center of the detected object, then adopted the objectness output as the adversarial loss, which experimentally shows it superior to the classification output; NPS loss and TV loss are also used to ensure the printability and naturalness of the adversarial patch. To improve the physical robustness of the adversarial patch, the author adopted a series of random transformations to the optimization process. Experiment results demonstrated that the generated adversarial patch could hide the person in front of the surveillance camera (based on YOLOv2) in most cases. However, there also exists the failure case when rotating the rotation in a large margin.

Zhao *et al.* [85] systemically investigated the adversarial patch attack against two detectors (i.e., YOLOv3 and Faster RCNN) in both digital and physical environments. Specifically, the author first exploited the intermediate features to enhance the adversarial examples. To enhance the physical adversarial attack, the author constructed a physical dataset by collecting the real-world background and traffic sign image, respectively; then, the traffic sign image is embedded into the background image. The author also adopted the EOT to guarantee the robustness of the adversarial patch. The author conducted the physical attack by placing the camera device inside the car and toward the printed adversarial patch. They evaluated different distances between the car and the adversarial patch by controlling the car's speed (i.e., $6\text{km/h} \sim 30\text{km/h}$), the attack success rate over 72%.

Unlike generating the adversarial patch to overlap the object for misclassified or misdetection, Lee *et al.* [86] introduced an

approach to craft the adversarial patch that can place anywhere (even far from the object) in the image, which can suppress all the detected objects. Specifically, the author designed the adversarial loss against the YOLO serial detectors and adopted the EOT (affine transformation and brightness on HSV color space) to improve the physical robustness. The PGD [12] is adopted to optimize the adversarial patch. In physical attacks, the author printed out the adversarial patch and recorded the video under natural lighting conditions. The YOLOv3 is adopted to evaluate the effect of physical attacks. Experiment results show that the patch is invariant to location. However, when placing the adversarial patch away from the object, the size of the patches needs to be enlarged.

4) *UPC*: Previous works mostly craft the instance perturbations for rigid or planar objects (e.g., traffic sign), ignoring the non-rigid or non-planar objects (e.g., clothes). To address this issue, Huang *et al.* [48] proposed to craft the universal physical adversarial camouflage (UPC) for the non-rigid object (i.e., person). Specifically, the author used the nature image as the initialization of the adversarial patch for the purpose of visual inconspicuous. Moreover, a set of transformations is performed on the adversarial patch to mimic deformable properties. Then, the author devised specific two-stage attack procedures against Faster RCNN: the RPN attack and the classifier and regressor attack, which are implemented by the following loss function.

$$\begin{aligned}\mathcal{L}_{rpn} &= \mathbb{E}_{p_i \sim \mathcal{P}} (\mathcal{D}(s_i, s_t) + s_i \|\vec{d}_i - \nabla \vec{d}_i\|_1), \\ \mathcal{L}_{cls} &= \mathbb{E}_{p_i \sim \hat{\mathcal{P}}} C(p)_y + \mathbb{E}_{p_i \sim \mathcal{P}^*} \mathcal{L}(C(p), y), \\ \mathcal{L}_{reg} &= \sum_{p_i \sim \mathcal{P}^*} \|R(p) - \nabla \vec{d}\|_2,\end{aligned}\quad (17)$$

where s_i and \vec{d}_i are the confidence score and coordinates of i -th bounding box; s_t is the target score, where s_1 and s_0 represent the background and foreground. $\nabla \vec{d}_i$ is the predefined vector that guides the optimization direction. C and R are the prediction output of the classifier and the regressor. P is the output proposal, $\hat{\mathcal{P}}$ is the top-k proposal filtered by confidence score and \mathcal{P}^* is the proposal that can be detected as true label y . \vec{d} denotes the distortion offset. Additionally, the TV loss is also adopted to produce more natural patterns. In physical attacks, the author printed the adversarial patterns and stuck them over the car (i.e., non-plane objects) and captured the picture from different distances (8 ~ 12 m) and angles ($-45^\circ \sim 45^\circ$). Experiment results show that the adversarial camouflage could reduce the detector's performance by a large margin.

5) *LPA Attack*: Unlike the previous patch-based physical attacks [45], Yang *et al.* [87] proposed to generate the adversarial license plate to fool the SSD. Specifically, the author devised a mask to guide the perturbation region, optimized by the C&W adversarial loss and color regularization consisting of NPS and TV loss to ensure adversarially and eliminate the color discrepancy between the digital and physical worlds. In optimization, EOT is used to enhance physical robustness. In physical attacks, the author created the adversarial license plate and placed it on the real car. Experiment results suggested

that the detection performance on captured images average degraded 76.9% in indoor and outdoor conditions.

6) *TranslucentPatch*: Unlike crafting the adversarial patch and pastes on the object's surface, Zolfi *et al.* [88] proposed a novel adversarial attack that crafts the adversarial patch, which was stuck on the camera lens. To avoid the camera lens being overlapped by the adversarial patch, the author took the image's alpha channel into account during the optimization. The author implemented the targeted attack and simultaneously maintained the non-attacked objects were not to be affected, which are implemented by the Equation (18) and (19).

$$\mathcal{L}_{target\ conf} = Pr(objectness) \times Pr(targetclass), \quad (18)$$

$$\begin{aligned}\mathcal{L}_{untarget\ conf} &= \frac{1}{M} \sum_{\substack{cls \in image \\ cls \neq target}} \\ &|conf(cls, clean) - conf(cls, patch)|,\end{aligned}\quad (19)$$

where the $Pr(objectness)$ and $Pr(class)$ represent the objectness and classification of detector, respectively. Additionally, the author also takes the Intersection over Union (IOU) as the adversarial loss

$$\mathcal{L}_{IoU} = IOU_{predcit}^{gt}(target). \quad (20)$$

The predicted bounding box changed by minimizing the \mathcal{L}_{IoU} . The author also adopted the NPS to ensure the color of the printed adversarial patches. The author conducts the physical attack by first printing out the adversarial patch on transparent paper, then placing it on the camera's lens, then capturing the video. The physical attack evaluated on YOLOv2/5 and Faster RCNN achieves over the average fooling rate of 35.48%.

7) *SwitchAttack*: Recently, Shapira *et al.* [89] developed a targeted attack method to generate the adversarial patch that is pasted on the car hood to attack object detectors (i.e., YOLOv3 and Faster RCNN) in a more realistic monitor scenario. Specifically, the author devised a tailored projection method to adaptively adjust the position and shape of the adversarial patch in terms of the camera orientation. To perform the targeted attack, the author considers all candidates that surpass the specific threshold before the NMS component to ensure the relevant candidates can be classified as the target label. Moreover, TV loss is adopted to improve the physical deployable of the adversarial patch. In physical attacks, the author stuck the printed patch on the toy car, achieving an attack success rate of 95.9% on recaptured images.

8) *ScreenAttack*: The first step of current patch-based physical attacks is to print out the adversarial patch, which is static in practice, and ignore the constantly changing character of the physical world, which may result in a failed attack. To address this challenge, Hoory *et al.* [90] proposed a dynamic adversarial patch for evading object detection models by displaying the adversarial patch with a digital screen (see Figure 11). The author adopted the loss function as the same to [47] to train the adversarial patch. Additionally, the author pointed out that the adversarial patch crafted by loss function

[47] is easily misdetected to the semantically related category, which makes it inconsistent with background objects. To this end, the author considered the semantically-related class (e.g., bus or truck) of the original class (i.e., car) as the target and devised the following loss function

$$J(\delta, x_{adv}, C) = \alpha \cdot TV(\delta) + \sum_{y_i \in C} \mathcal{L}(f(x_{adv}), y_i), \quad (21)$$

where C is the set of semantically-related labels used to avoid being detected as car-related classes. Furthermore, the author split the train set into multi subsets and trained an adversarial patch for each subset. In physical attacks, the author placed a digital screen on the side and rear of the car, where the adversarial patch is chosen from the patch subsets to dynamic display in terms of the changing environmental conditions. Evaluation results on YOLOv2 suggested that 90% video frames with the adversarial perturbed screen can not detect the target object (i.e., car).

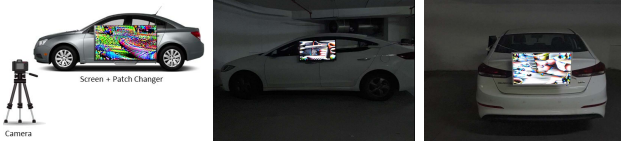


Fig. 11. Dynamic attack by display the adversarial patch on the screen. [90]

Recently, the adversarial patch has been applied to attack the face detector (i.e., FPN [120]) in the digital domain ([121]) by sticking on the person's forehead to conduct the adversarial attack.

B. Wearable adversarial perturbation

Unlike devising the simple plane (non-rigid) adversarial perturbation, the non-rigid object show more difficult as that needs to take the deformable of the adversarial patch into account in physical deployable. Wearable adversarial perturbation approaches [91], [92], [92], [93] were designed to address that issue. Figure 12 illustrates the related wearable patch-based adversarial attack.

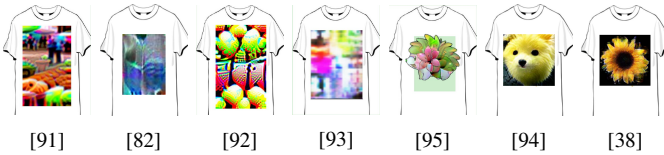


Fig. 12. Visualization examples of various wearable adversarial patches.

Yang *et al.* [91] extended EOT from 2D space to 3D space by building up a pinhole camera model to mimic the patch's transformation in the physical world. In optimization, the author adopted the C&W-based adversarial loss, TV loss, and Euclidean distance between the clean image and the adversarial image with patch to optimize the adversarial patch. In physical attacks, the author holds the laptop where the screen displays the adversarial patch. Experiment results on the captured image show that the YOLO's detection performance degraded from 100% to 28%.

Xu *et al.* [92] proposed an adversarial T-shirt attack to avoid the detection of the single object detector (i.e., person) in the physical world. The generated adversarial pattern is attached to the surface of the T-shirt. To mimic the cloth deformation in the physical world, the author proposed to apply the Thin Plate Spline Mapping (TPS) transformation over the adversarial perturbation. To further enhance the performance of the adversarial attack, the author adopted the following three approaches: 1) approximate the cloth's deformation with TPS; 2) approximate the color discrepancy between digital and physical space with a quadratic polynomial regression. 3) enhance the robustness of the adversarial perturbation with EOT. By performing the above operations, the T-shirt stuck with the adversarial patch degrades the person detector significantly under indoor and outdoor physical conditions.

Concurrent to [92], Wu *et al.* [93] proposed to devise an adversarial patch to implement the disappear attack. To this end, the author devised the objectness disappear loss, which is expressed as follows

$$\mathcal{L}_{obj} = \mathbb{E}_{t \sim \mathcal{T}} \sum_i \max \{S_i(A(x, \delta, t)) + 1, 0\}^2, \quad (22)$$

where $A(x, \delta, t)$ is the patch apply function, which pastes the adversarial patch δ on the image with the transformation process t ; S_i indexes the objectness score of i -th proposal. By minimizing this loss function, the adversarial examples with the devised patch could suppress the positive scores. Additionally, the TV loss is adopted to ensure the visual effect of the adversarial patch. In physical attacks, the author treated the printed patch as a sticker of the clothes. Experiment results suggest that the adversarial patch in the physical world could deceive the YOLOv2 and Faster RCNN. Moreover, the author empirically finds that the TPS would detriment the adversarial performance.

Tan *et al.* [94] pointed out the existing adversarial wearable patches are conspicuous to humans. Thus, the author proposed two-stage strategies to optimize the legitimate adversarial patch that can evade both human eyes and detection models in the physical world. In the first stage, the author began with a random cartoon image and optimized an adversarial patch that could deceive the detector. In the second stage, the author adopted the clean cartoon image and the optimized patch crafted in the first stage to constrain the adversarial patch to evade human attention. The author adopted the TV loss and the Euclidean distance between the adversarial patch and the cartoon image to ensure visually natural to human observers. Moreover, NPS loss is used to constrain the patch color inside the printable colors. The author conducted the physical attack by attaching the printed adversarial patch to the white T-shirts. The case study shows the effectiveness of their adversarial patch against YOLOv2 in the physical attack.

Concurrently to [94], Hu *et al.* [95] proposed to exploit the learned image manifold of a pre-trained GAN (e.g., BigGAN and StyleGAN) to guide the adversarial patch generation. Rather than directly optimizing the adversarial patch from scratch, the author treats the image sample sampling from the generator as the adversarial patch. Then the patch is

applied to the target object inside the image to constructing the adversarial examples. The TV loss and the following adversarial loss are adopted to optimize the adversarial patch

$$\mathcal{L} = \frac{1}{N} \sum_{i=1}^N \max_j [f_{obj}^j(x_{adv_i}) \cdot f_{cls}^j(x_{adv_i})], \quad (23)$$

where the x_{adv_i} is the i -th image in a batch with size N . f_{cls}^j, f_{obj}^j represent the class probability and objectness probability, respectively. In physical attacks under indoor and outdoor conditions, the author recorded one person wearing the adversarial shirt side-by-side with another person wearing an ordinary shirt. Experiment results show that the physically recaptured image could degrade the detection recall of YOLOv4tiny by approximately 23.80% and 43.14% (for indoor and outdoor, respectively). Moreover, they exhaustively investigate the influence of different transformations, patch sizes, and target classes on attack performance.

Hu *et al.* [96] got inspiration from cloth making and proposed to treat the adversarial patch as the whole cloth to be cut. To generate a naturalistic patch, the author utilized the generative model to generate the adversarial patch and then overlap them with the object. To simulate the physical deformation of the cloth, the author applied the TPS transformation over the adversarial patch. TV loss is adopted to ensure the smoothness of the patch's pattern. They conduct the physical experiment by painting the adversarial patch over the cloth and then making the clothes. The adversary who wore the crafted adversarial clothes can bypass the detector with the average attack success rate of 80.75% against different detectors (i.e., YOLOv2/3, Faster RCNN, and Mask RCNN) under different distances and view angles (range from 0° to 180°). Figure 13 describe the adversarial patch and the corresponding clothes.

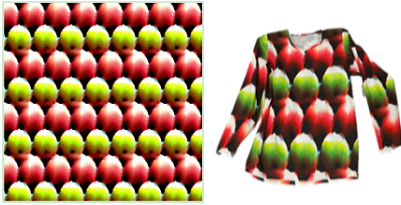


Fig. 13. Adversarial patch (left) v.s. adversarial clothes (right). [96]

C. Projector's Projection

Rather than generating the adversarial patch directly, Lovisotto *et al.* [97] presented a novel adversarial attack by modulating the projector's parameters. The author first collected the projectable colors as following step: 1) collect the target image of the target object as the projection surface S ; 2) select a color $c_p = [r, g, b]$, and the color P_{c_p} over the projection surface, resulting in the output O_{c_p} . Finally, repeat the above two steps until collecting enough data. The author takes the camera noise and projector's work mechanism into account to collect the realistic color as possible. After that, the author fitted a projection model as follows

$$\mathcal{L}_{\mathcal{P}} = \operatorname{argmin}_w \sum_{\forall c_s, c_p} \|\mathcal{P}(c_s, c_p) - c_o^{(s,p)}\|_1, \quad (24)$$

where \mathcal{P} is the projection model, $c_s, c_p, c_o^{(s,p)}$ is the training data triple, consists of projecting c_p on pixels of color c_s , and the output $c_o^{(s,p)}$; w is the parameters of the projection model. To optimize the adversarial examples, the author combined the EOT and treated the objectness and classification output of the detector as the adversarial loss. The author conducted the physical attack by placing the projector away from the target object from 1 to 12 meters and viewing angles $-30^\circ \sim 30^\circ$, achieving the success rate 100% for the traffic sign classification model and 77% for object detectors (i.e., Mask RCNN and YOLOv3).

D. Camouflage-based physical adversarial attack

The works discussed above are mainly focused on generating the adversarial patch on the 2D image, where each pixel can be modified independently. Recently, researchers have increasingly paid attention to more realistic attacks in 3D space, developing adversarial camouflage-based attacks that focus on modifying the appearance (i.e., shape or texture) of the 3D object.

1) *Shape of 3D object*: Zeng *et al.* [98] first proposed to generate the adversarial examples against 3D shape classification and a visual question answer (VQA) system. Specifically, they crafted the adversarial example by adopting the neural renderer technique, which allows them to perform the 3D transformation to better approximate real-world environments. Concurrent to Zeng [98], Xiao *et al.* [122] proposed to generate an adversarial object by modifying the mesh of a 3D object, namely MeshAdv. The adversarial mesh is optimized on the total loss consisting of classification loss, objectness loss, and perceptual loss. Moreover, the author extends the TV loss from pixel-wise in the 2D image to the vertex in the 3D image. However, the methods of the above method limited their utilization, which made them fail to conduct the physical attack.

2) *CAMOU*: Unlike the works [98], [122] optimize the object mesh, Zhang *et al.* [99] proposed to optimize the texture of the 3D object. The author presented a clone network to mimic the entire processing containing the adversarial texture render and detector prediction. Then apply the white-box attack on the clone network to optimize the adversarial texture. Although the camouflaged vehicle achieved good attack performance on Mask RCNN, the optimized texture is a mosaic-like pattern, which is conspicuous to the human observer.

3) *UPC*: Huang *et al.* [48] proposed to optimize the adversarial texture from the patch seed and stick the adversarial patch over the partial vehicle's surface to obtain well appearance. It is worth noting that the author printed out the adversarial texture and stuck it on the real car to experiment.

4) *ER*: Rather than construct the adversarial patch under the white-box setting, Wu *et al.* [100] considered a more challenging black-box attack. The author proposed to utilize the genetic algorithm to optimize the adversarial texture. To reduce the optimization variable, the author optimizes small-size adversarial texture (64×64), then enlarges or repeats (ER) to a large scale (2048×2048). The adversarial texture is rendered wrapped over the vehicle in the simulator environment via Carla [123] PythonAPI, then recorded the adversarial

examples from the simulator environment and used to query the detector (i.e., Light head RCNN [124]). They show the adversarial texture generated by the black-box attack could significantly reduce the performance (the magnitude of 52%) of the detector in the simulator environment while ignore verify the physical attack.

5) *DAS*: Wang *et al.* [30] pointed out that the adversarial camouflage generated by the previous works [99], [100] failed to consider the model's attention, resulting inferior transferability. To this end, the author proposed simultaneously suppressing the model and human attention. To suppress the model's attention, the author proposed dispersing the intensity attention map by disconnecting the connected graph generated from the attention map. To suppress human attention, the author adopted the seed content patch as initialization and encouraged the adversarial texture to remain similar to the seed content. Moreover, the author optimizes the specific part faces of the 3D model as the textures via neural renderer [125]. To optimize the adversarial texture, the author constructed a dataset sampled from the Carla simulator at different distances and angles. The author conducts the physical attack by printing out the camouflaged rendered car on paper and then cropping the camouflage texture and sticking it on the toy car. Experiment results suggested that the average performance reduction of four detectors (i.e., YOLOv5, SDD, Faster RCNN, and Mask RCNN) is 26.05%.

6) *FCA*: Recently, Wang *et al.* [33] proposed to craft the full-coverage adversarial camouflage texture to overcome more complex environment conditions (e.g., multi-view and occlusion), which are less explored in the current patch-like [47] and partial camouflage work [30], [48]. To maintain the effectiveness of the small ratio of adversarial camouflaged vehicles in the image, the author used multi-scale IOU loss to constrain the adversarial texture. Finally, the author combined the TV loss and adversarial loss (i.e., including IOU, classification, and objections) to optimize the adversarial camouflage texture. They adopt a similar physical attack process (including datasets and detector) with [30], and the experiment shows their method's effectiveness under complex environments, degrading the average reduction of the detector performance of 53.99% in physical attacks.

7) *CAC*: Unlike [33] optimize the full coverage faces of the 3D model that encountered the difficult issue of hard implementation, Duan *et al.* [34] proposed to optimize the 2D texture of the 3D model directly. They proposed to optimize the texture by minimizing all classification output of the RPN module at the first stage of Faster RCNN. Although they adopted various physical settings (e.g., angles, brightness, etc.), the author trained the texture on the image with pure-color background. In physical attacks, the author print out the entire vehicle model with the 3D printer, and the experiment demonstrates their method's effectiveness in the physical environment under 360° free viewpoint settings.

8) *DTA*: Suryanto *et al.* [35] pointed out the previous works [30], [33] fail to consider more specific physical environmental conditions, e.g., shadow. To address the above issue, the author used a network to approximate the shadowing effect. Rather than adopt the neural renderer to optimize the adversarial

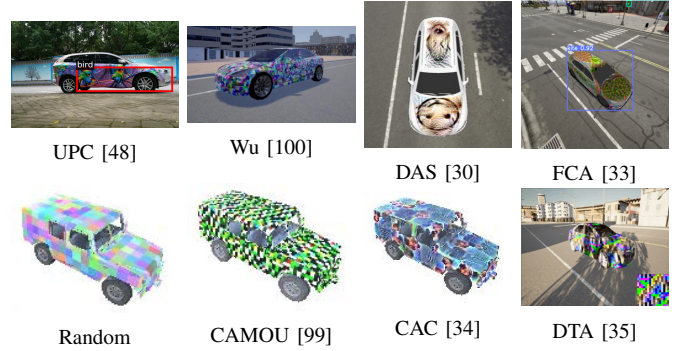


Fig. 14. Visual appearance of various camouflage texture rendered vehicle.

texture, the author optimizes the 2D image as the texture but transforms them with the same camera matrix as the vehicle. In physical attacks, the author printed out the camouflaged 3D object with a 3D printer and captured the photo every 45°. Experiment results suggested that the average performance reduction of two detectors (i.e., EfficientDetD0 [126] and YOLOv4) model is 47.5%.

In summary, the camouflage-based adversarial texture has attracted increasing attention in recent years because it can better mimic physical transformations (e.g., shadowing and brightness). For example, recently, Byun *et al.* [127] proposed to adopt the neural renderer as the data augmentation technique to boost the robustness of adversarial examples. The discussed camouflaged attacks mainly focus on generating the adversarial camouflage texture, while the loss function, especially adversarial loss, has been less explored. Additionally, these works conducted the physical attack by printing a small-size car model rather than the real car. We argue it is far away from a realistic attack on the vehicle. Alcorn *et al.* [128] argued that the reason for the vulnerability of detectors might be attributed to these simulated images being strange to the detector. In other words, the detector was not trained on such simulated data, resulting in bad generalization. Moreover, there are many issues to be solved, including but not limited to small-size adversarial objects and the complex physical environment condition (e.g., occlusion and lighting) in the real world.

E. Against the infrared detectors

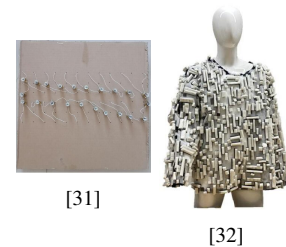


Fig. 15. Adversarial against infrared thermal imaging detector.

The existing physical adversarial attack mainly focused on the RGB image in visible light, while visible light has its limitations in dark environments (e.g., darkness); for example, the image content taken in the evening is hardly identified. However, infrared thermal imaging has its advantage because

it is free from lighting changes, enabling them adopted widely in the real world.

Zhu *et al.* [31] proposed a novel adversarial method to attack the infrared thermal imaging detector. The author devised a board with multi bulbs, where the positions of bulbs are the optimization variables. To mimic the shining of the bulb, the author applied the gaussian function on the pixel of the bulb's position. Finally, the author treated the combination of objectness output of detector and TV loss as their loss function to optimize the adversarial patch. The author conducted the physical attack by placing the bulb in the optimized positions and photoed the people who held the board. Experiment results show that the adversarial bulb board degrades the detector by 34.48%.

Recently, the author pointed out that [31] may be failed in multi-view environments and proposed to construct the adversarial clothes covered with adversarial texture made by aerogel [32]. More specifically, the author adopted a similar idea with [96] to optimize the adversarial patch image. To simplify the physical implementation, the author optimized the QR code-like adversarial texture, which allows the author only required to optimize the generation parameters of the QR code texture. The generated QR code texture is tiled to a large shape, and then the actual adversarial patch is randomly cropped from the tiled image and then pasted onto the target object in the image. The TPS and various transformations are used to improve the robustness of the adversarial patch. The author made the clothes by attaching the black block to the aerogel according to the optimized QR code texture. The participant who wore the adversarial patch could successfully bypass the detector (i.e., YOLOv3), where the detection performance degraded by 64.6%.

F. Against Aerial detection

Unmanned aerial surveillance has gained increasing attention with the development of drone techniques and object detection. Correspondingly, the adversarial attack against unmanned aerial surveillance aroused increasing attention in the military scenario. The conventional technique against unmanned aerial surveillance is to use the camouflage net, while a recent study shows that a partial imagery patch could deceive the unmanned aerial surveillance.

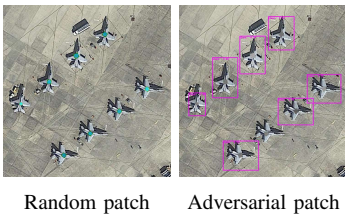


Fig. 16. Visualization result of different patch. [129].

Den Hollander *et al.* [129] assumed unmanned aerial surveillance is the YOLOv2 trained on the aerial imagery dataset. To attack the object detector, the author combined the common loss consisting of the adversarial loss, NPS loss, and the objectness loss and proposed a novel colorfulness metric

as a saliency loss to train the adversarial patch. The saliency loss is represented as follows

$$\mathcal{L}_{sal} = \sqrt{\sigma_{rg}^2 + \sigma_{yb}^2} + 0.3 * \sqrt{\mu_{rg}^2 + \mu_{yb}^2} \quad (25)$$

$$rg = R - G, yb = 0.5 * (R + G) - B,$$

where μ and σ are the averages, and the standard deviation of the auxiliary variables, R, G, and B denote the patch's color channel values. The author investigated the impact of the patch's size, position, number, and saliency on the adversarial performance. Experiment results demonstrate that the optimized patch could reduce the detector performance significantly (i.e., 47%).

Recently, Du *et al.* [101] implement the physical adversarial attack against the aerial imagery detection. Considering the realistic scenario, the author designed two types (see Figure 17) of adversarial patches to accommodate the different scenarios. Type ON refers to the adversary placing the adversarial patch on the top of the car, which is suitable for dynamic scenarios (i.e., the car is driving). By contrast, Type OFF refers to the adversary placing the adversarial patch around the car, which is suitable for stationary scenarios (e.g., parking lot). The author adopted objectness, NPS, and TV loss to train the adversarial patch. The author conducted the physical attack by printing out the adversarial patch and placing them around or near the target objects under different lighting conditions. Experiment results demonstrated that the printed-out adversarial patch could significantly reduce objectness score (25% to 85%).

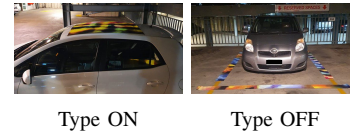


Fig. 17. Patches designs [101].

Apart from two adversarial patch attacks against the object detector on the aerial imagery dataset, there are a number of attempts to attack the remote sensing image recognition, and detection [130]–[132].

G. Other adversarial attacks against object detection

Although physical attacks consider the more realistic conditions, the basic procedure behind physical attacks is similar to digital attacks, i.e., the first step of the physical adversarial attack is to construct the adversarial perturbation in the digital world. Thus, some digital attacks may inspire physical attacks. Wang *et al.* [133] proposed a dense adversarial generation (DAG) attack, which simultaneously attacks the classification, objectness, and the classification and regress loss of the RPN module. Chow *et al.* [134] systemically investigate the adversarial objectness attack against the common detectors (i.e., YOLOv3, SSD, and Faster RCNN) on three different benchmark datasets, the devised adversarial patch could paste on the image or add into the image. Wang *et al.* [135] proposed a creative attack by disturbing the non-maximum suppression (NMS) module of the detector, which resulted in enormous wrong results on the generated adversarial examples. Liao *et*

al. [136] showed that there is no need to generate global perturbation for the whole image, the author exploited the high-level semantic information to generate local perturbation for detectors. To improve the naturalness of the adversarial patch, Pavlitskaya *et al.* [36] extend the existing GAN-based approaches [95] by attacking all object that appears in the image to generate inconspicuous patches, and then assessed the trade-off between attack performance and naturalness.



Fig. 18. Visualization of different sparse attack against the object detector.

Unlike searching the global perturbation for the whole image, the research has attempted to implement the sparse attack by perturbing a few numbers of the image pixel, which makes them suitable for extending to physical attacks. Although the sparse adversarial attack has been investigated in image recognition systems [140]–[144], their application on object detection is unexplored. Figure 18 illustrated the successfully sparse adversarial attack in the digital world.

To perform the sparse adversarial attack, Bao *et al.* [137] generated the adversarial patch by simultaneously considering the position, shape, and size of the adversarial patch into optimization. Zhao *et al.* [145] proposed two adversarial patch generation algorithms: exploit the heatmap to guide the patch application and consensus-based algorithm (i.e., one of the model ensemble strategies). The proposed algorithm won seventh place in the Alibaba Tianchi adversarial challenge object detection competition. Wu *et al.* [138] proposed a diffused patch attack to optimize the adversarial line embedded in the object’s center. The proposed attack won second place in the Tianchi competition. Li *et al.* [146] extend the universal adversarial perturbation [147] from image recognition tasks to object detection tasks and proposed a universal dense object suppression (U-DOS) algorithm to optimize the universal adversarial perturbation to deceive the detector on most input images. To probe the model’s blind spots, Zhu *et al.* [148] came up with a novel approach that simultaneously models the shape and the pattern of the adversarial patch; they can generate multi patches with different shapes for a specific image. Huang *et al.* [139] proposed to generate the adversarial patch and gradually remove the inconsequential perturbation in the crafted patch. In addition, the author devised a weighted strategy to stabilize the model ensemble, avoiding the countermeasure among different detectors. The experiment result shows that perturbing a few numbers of pixels could reduce the detector significantly (obtaining 100% missed detection

rate for both YOLOv4 and Faster RCNN).

H. Attack Semantic Segmentation

Semantic segmentation is similar to the object detection task but needs fine-grind classification for every pixel in the image. However, physical attacks against semantic segmentation are less explored, which will be discussed as follow.

Nesti *et al.* [102] proposed to optimized a scene-specific billboard patch to attack the semantic segmentation models. The author exploits the Carla simulator [123] to simulate a more realistic environment of the real world. Rather than adopt the EOT in the 2D image space, the author exploited various physical transformations in the 3D dimension provided by Carla. More specifically, the author first applied the projective transformation to precisely paste the patch onto the 2D attackable surface with the extracted 3D rotation matrix. The author devised the following loss function to optimize the patch.

$$\mathcal{L}_M = \sum_{r \in \Omega} \mathcal{L}_{CE}(f_i(x_{adv}), y_i), \mathcal{L}_{\bar{M}} = \sum_{r \notin \Omega} \mathcal{L}_{CE}(f_i(x_{adv}), y_i), \quad (26)$$

where \mathcal{L}_M describes the cumulative cross entropy (CE) for those pixels that have been misclassified with respect to the ground truth y , denoted as Ω ; while $\mathcal{L}_{\bar{M}}$ refers to all the others. The author printed out the billboard patch as a 1×2 meter poster, which could successfully hide the target object. Figure 19 illustrates the physical billboard patch.

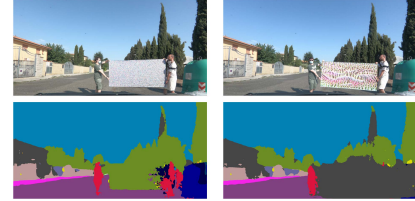


Fig. 19. Visualization of Random patch (left) and optimized patch (right). [102]

Unlike the image recognition and object detection task, the research on the physical adversarial attack against the semantic segmentation task lacks enough attention. The possible reason is the task similarity between object detection and semantic segmentation. Additionally, semantic segmentation models are commonly deployed in autonomous driving, and the physical adversarial attack against the autonomous driving system has gained enormous attention [149]–[151], which is beyond the discussion of this paper. Such reason may result in a few numbers of literature investigating the physical adversarial attack against semantic segmentation.

Nonetheless, several attempts have explored the digital attack against semantic segmentation. Hendrik Metzen *et al.* [152] proposed universal adversarial perturbation to deceive the semantic segmentation on most images. Unlike to [152], Nakka *et al.* [153] pointed out there is no need to perturb the whole image to realize the attack and proposed to optimize the adversarial patch applied to the object to attack the semantic segmentation. Arnab *et al.* [154] systematically investigated

the adversarial robustness of the semantic segmentation with respect to various attack (e.g., FGSM [10], PGD [12]).

Additionally, physical adversarial attacks have been recently applied to various fields, such as depth estimation [103] and object tracking [104], [105].

VI. DISCUSSION AND FUTURE WORK

Although physical adversarial attacks impose potential risks for existing deployed DNN-based systems, the issue remains to be solved. In this section, from the perspective of the attack pipeline (i.e., input transformation, algorithm design, and evaluation), we will summarize the common techniques used to develop physical attacks and then discuss the promising methods used to boost further the performance of physical attacks. Finally, we discuss the potentially beneficial application of the physical deployable adversarial perturbation.

A. Input transformation

The essential of input transformation is the expectation maximization of the objective function over the inputs that convert on various transformation operations (e.g., rotation, affine transform, brightness adjust). In adversarial attacks, the transformation is exerted on the adversarial examples to make them robust to such transformation or boost their transferability. Thus, input transformation is a simple but effective way to improve adversarial attacks' performance both in the digital and physical world. However, the complex environmental condition may curb the effectiveness of such transformations. To address the issue, the digital and the corresponding physical recaptured image pairs are used to boost the physical robustness of adversarial perturbation. Another solution is to use a network to model the discrepancy between the digital and physical worlds.

To better mimic the physical transformation in the real world, given the stronger learning capability of DNN, one approach is to exploit a network to learn the various physical transformation, such as shadow, brightness, rotation, saturation, and so on. For example, one can use a network to learn the explicit physical transformation from video sequences. Thus, collecting high-quality training data is significant to the network's performance.

B. Attack algorithm design

Although a line of physical attacks has been proposed for different tasks and achieved certain success, many problems still exist, which will be discussed as follows.

1) *Adversarial patch application*: Adversarial patch application refers to how to paste the adversarial perturbation on the host image/object, which is crucial for adversarial patch attacks. However, most existing works have used the mask to guide the application of the adversarial patch, which curbs the performance of the attacks. The reason may include two-fold: on one side, only a specific area of the image is crucial for the model decisions, and modifying unspecific areas may have a countereffect; On another side, a large block of perturbation is conspicuous to the human observer, hurting its stealthiness.

Based on the aforementioned discussion, one promising approach is to adaptive adjust the mask's shape, such as using a network to automatically learn the best mask or exploit the geometry algorithm to optimize the optimal mask.

2) *Universal adversarial perturbation via black-box attack*: Many existing physical attacks belong to white-box attacks, and the perturbation is defaulted to be universal, which means it only requires optimizing one perturbation to fool the whole dataset. Despite their success, the white-box setting is not practical in practice. Regarding black-box attacks, there are plenty of works [16], [155]–[157] have been proposed for attacking the target model in the digital world. Moreover, these works are designed to generate perturbation for each input image, which limits their application in practice. In surveyed works, only one work was proposed to optimize the universal adversarial perturbation against the image recognition model in digital work [158].

Therefore, developing physically deployable universal black-box attacks is more realistic in practice but more difficult. Some algorithms can solve the above problem, such as genetic algorithm, differential evolution, particle swarm optimization, and random search. However, optimizing the perturbation revolves to solve a high-dimension optimization problem, which significantly confines the efficiency and effectiveness of the attack. Thus, reducing the optimization dimension is crucial for developing the physical deployable black-box attack. Moreover, other issues referring to black-box may need to be considered, such as time-consuming and query efficient.

3) *Transferability*: Transferability is one of the significant characteristics of adversarial perturbation, which refers to the adversarial perturbation generated for the known model and can also be used to attack the unknown model. In realistic physical attacks, the adversary may not know what the DNN deployed in the system, which makes the transferability of adversarial perturbation essential for physical attack performance. However, the existing physical attacks mainly focus on the robustness of physical attacks and attack performance on specific known models, making the transferability of physical adversarial attacks less explored.

There are enormous works attempts to improve the transferability of digital attacks, including but not limited to input transformation, gradient calibration, feature-level attack, model ensemble, and generative model. These techniques could be combined with physical attacks to boost their transferability.

4) *Simultaneous attack multitask*: Most current physical attacks focus on attacking specific tasks, such as image recognition and object detection. However, in the real world, the attacker cannot get knowledge about the target victim system, such as whether the system is equipped with the image recognition model or object detection model. Therefore, one promising direction to address the above problem is to take multi-task into account during the optimization simultaneously.

Recently, the vision transformer (aka., ViT) provided a novel general framework for vision tasks, exhibiting competitive performance to CNN-based framework. With the increasing

application of ViT, physical adversarial attacks against the ViT should arouse the researcher's attention.

5) *Robustness of physical attacks*: The main problem faced by physical adversarial attacks is the complex physical environments, including brightness, lighting, shadow, deformation, distance, occlusion, and the system noise introduced by the imaging sensor (i.e., camera). The existing approaches encounter the following drawbacks when applied to physical attacks. First, they generally resit some of these conditions and hard take all underlying physical environment factors into account. Second, they cannot cover some physical conditions, such as partial shadow or occlusion of the target object. Third, the used transformation (e.g., rotation or brightness change) modifies the whole pixel of the image instead of the target object, which is inconsistent with real physical deployment. Finally, there are no works to take the dynamic changing of the size of the target object into account, which is crucial in the real-world scenario as the perturbed object will move. Therefore, constructing a general and robust physical adversarial attack is an open problem for future research.

Two promising techniques may be can used to solve the above issues. The first one is to utilize the technique from the computer graphic, such as the physical renderer, a computer graphics approach that seeks to render images in a way that models the flow of light in the real world. The second one is to utilize emerging technologies, i.e., neural radiance fields (NeRF), a method for synthesis for novel views of complex scenes. The abovementioned approaches can be integrated into optimizing adversarial attacks to mimic complex real-world conditions.

6) *Stealthiness*: Most existing successful physical adversarial attacks pursue higher and more robust attack performance with the sacrifice of perceptible. One reason is the mode of projecting the perturbation to the sphere of L_∞ with a radius of a specific magnitude in digital attacks may be unsuitable for physical attacks as the slight perturbation may be distorted caused by the device noise or environmental factors, making the attack invalid. Moreover, visually conspicuous adversarial perturbation patterns easily observe by humans. Thus, as we cannot diminish the perturbation magnitude, making the adversarial patterns more natural may be a promising work.

C. Evaluation

1) *Evaluation benchmark dataset*: Although most physical attack methods were proposed, they are devised for different datasets, resulting in hardly evaluating different methods on one uniform dataset. Thus, it is urgent to develop a public dataset for evaluating the effectiveness of the attack methods. On the other hand, there is no unified evaluation process and criterion for physical attacks, which makes it hard to reproduce the result reported in the publications. However, the real environment is complex and hard to reproduce as the changing weather and light condition. Recently, some research has attempted to use the simulator to develop adversarial attacks, which gives a promising direction to develop an environment for evaluating physical attacks as the simulator can provide reproducibility and definite environments by fixing

the scene and parameters (e.g., weather and light conditions). For example, one can develop a physical testing environment using an open source simulator (e.g., Carla [159] or AirSim [160]), then provide the physical testing interface, allowing the attacker to call the testing procedure with their optimized adversarial perturbation and report the attack results.

2) *Uniform physical test criterion*: Most physical attacks conduct physical experiments under stationary conditions, which means that the adversary takes photos of the adversarial perturbation disturbed object at a specific position and then evaluates the attack performance of the captured image. However, the target object moves in and out of the viewfinder of the system's sensor device in the actual physical environment, meaning that the ratio of the perturbed object is dynamically changing with respect to the fixed viewfinder. In the dynamically changing process, many factors caused by the background environment would impact the attack performance. The stationary test cannot include such a complex scenario. To this end, the dynamic physical test may better represent the performance of the attack method in the real world. Therefore, a complete criterion of the physical test process is urgent to boost the development of physical adversarial attacks.

3) *Applications*: The adversarial attack is a double-blade sword. On the one side, adversarial attacks would lead the DNN-based system to make mistakes, resulting in potential security risks. On the other side, adversarial attacks also have their benefits side, such as 1) the adversarial perturbed physical adversarial example could be used as the training data to boost the adversarial robustness of DNN further; 2) adversarial perturbation can used to help the DNN system remain stable in complex environmental conditions [161], [162]. Therefore, potential applications exploiting adversarial perturbation to boost the performance of DNN in the real world is an interesting research direction.

VII. CONCLUSION

In this paper, we systemically discussed the physical adversarial attacks in computer vision tasks, including image recognition and object detector tasks. We argue that DNN-based systems still face enormous potential risks in both digital and physical environments. These risks should be thoroughly studied to avoid unnecessary loss when widely deployed in the real world. Specifically, we proposed a taxonomy scheme to categorize the current physical adversarial attack to provide a comprehensive overview. By reviewing the existing physical adversarial attack, we summarize the common characteristic of physical adversarial attacks, which may be helpful to future physical adversarial attack research. Finally, we discuss the problems that need to be solved in physical adversarial attacks and provide some possible research directions.

VIII. ACKNOWLEDGMENTS

This work was supported by the National Natural Science Foundation of China (No.11725211 and 52005505).

REFERENCES

- [1] K. Simonyan and A. Zisserman, "Very deep convolutional networks for large-scale image recognition," *arXiv preprint arXiv:1409.1556*, 2014.
- [2] K. He, X. Zhang, S. Ren, and J. Sun, "Deep residual learning for image recognition," in *Proceedings of the IEEE conference on computer vision and pattern recognition*, 2016, pp. 770–778.
- [3] N. Carion, F. Massa, G. Synnaeve, N. Usunier, A. Kirillov, and S. Zagoruyko, "End-to-end object detection with transformers," in *European conference on computer vision*. Springer, 2020, pp. 213–229.
- [4] Z. Liu, Y. Lin, Y. Cao, H. Hu, Y. Wei, Z. Zhang, S. Lin, and B. Guo, "Swin transformer: Hierarchical vision transformer using shifted windows," in *Proceedings of the IEEE/CVF International Conference on Computer Vision*, 2021, pp. 10012–10022.
- [5] A. Vaswani, N. Shazeer, N. Parmar, J. Uszkoreit, L. Jones, A. N. Gomez, L. Kaiser, and I. Polosukhin, "Attention is all you need," *Advances in neural information processing systems*, vol. 30, 2017.
- [6] J. Devlin, M.-W. Chang, K. Lee, and K. Toutanova, "Bert: Pre-training of deep bidirectional transformers for language understanding," *arXiv preprint arXiv:1810.04805*, 2018.
- [7] D. Amodei, S. Ananthanarayanan, R. Anubhai, J. Bai, E. Battenberg, C. Case, J. Casper, B. Catanzaro, Q. Cheng, G. Chen *et al.*, "Deep speech 2: End-to-end speech recognition in english and mandarin," in *International conference on machine learning*. PMLR, 2016, pp. 173–182.
- [8] A. Gulati, J. Qin, C.-C. Chiu, N. Parmar, Y. Zhang, J. Yu, W. Han, S. Wang, Z. Zhang, Y. Wu *et al.*, "Conformer: Convolution-augmented transformer for speech recognition," *arXiv preprint arXiv:2005.08100*, 2020.
- [9] C. Szegedy, W. Zaremba, I. Sutskever, J. Bruna, D. Erhan, I. J. Goodfellow, and R. Fergus, "Intriguing properties of neural networks," in *2nd International Conference on Learning Representations, ICLR 2014, Banff, AB, Canada, April 14-16, 2014, Conference Track Proceedings*, 2014. [Online]. Available: <http://arxiv.org/abs/1312.6199>
- [10] I. Goodfellow, J. Shlens, and C. Szegedy, "Explaining and harnessing adversarial examples," in *International Conference on Learning Representations*, 2015. [Online]. Available: <http://arxiv.org/abs/1412.6572>
- [11] A. Kurakin, I. Goodfellow, and S. Bengio, "Adversarial machine learning at scale," *arXiv preprint arXiv:1611.01236*, 2016.
- [12] A. Madry, A. Makelov, L. Schmidt, D. Tsipras, and A. Vladu, "Towards deep learning models resistant to adversarial attacks," in *6th International Conference on Learning Representations, ICLR 2018, Vancouver, BC, Canada, April 30 - May 3, 2018, Conference Track Proceedings*. OpenReview.net, 2018.
- [13] Y. Dong, F. Liao, T. Pang, H. Su, J. Zhu, X. Hu, and J. Li, "Boosting adversarial attacks with momentum," *2018 IEEE/CVF Conference on Computer Vision and Pattern Recognition*, pp. 9185–9193, 2018.
- [14] N. Carlini and D. Wagner, "Towards evaluating the robustness of neural networks," in *2017 IEEE Symposium on Security and Privacy (SP)*. IEEE, 2017, pp. 39–57.
- [15] Z. Huang and T. Zhang, "Black-box adversarial attack with transferable model-based embedding," in *International Conference on Learning Representations*, 2020. [Online]. Available: <https://openreview.net/forum?id=SJxhNTNYwB>
- [16] C. Li, H. Wang, J. Zhang, W. Yao, and T. Jiang, "An approximated gradient sign method using differential evolution for black-box adversarial attack," *IEEE Transactions on Evolutionary Computation*, pp. 1–1, 2022.
- [17] L. Sun, M. Tan, and Z. Zhou, "A survey of practical adversarial example attacks," *Cybersecurity*, vol. 1, no. 1, pp. 1–9, 2018.
- [18] R. R. Wiyatno, A. Xu, O. Dia, and A. de Berker, "Adversarial examples in modern machine learning: A review," *arXiv preprint arXiv:1911.05268*, 2019.
- [19] S. Qiu, Q. Liu, S. Zhou, and C. Wu, "Review of artificial intelligence adversarial attack and defense technologies," *Applied Sciences*, vol. 9, no. 5, p. 909, 2019.
- [20] X. Yuan, P. He, Q. Zhu, and X. Li, "Adversarial examples: Attacks and defenses for deep learning," *IEEE transactions on neural networks and learning systems*, vol. 30, no. 9, pp. 2805–2824, 2019.
- [21] A. Serban, E. Poll, and J. Visser, "Adversarial examples on object recognition: A comprehensive survey," *ACM Computing Surveys (CSUR)*, vol. 53, no. 3, pp. 1–38, 2020.
- [22] K. Ren, T. Zheng, Z. Qin, and X. Liu, "Adversarial attacks and defenses in deep learning," *Engineering*, vol. 6, no. 3, pp. 346–360, 2020.
- [23] J. Zhang and C. Li, "Adversarial examples: Opportunities and challenges," *IEEE transactions on neural networks and learning systems*, vol. 31, no. 7, pp. 2578–2593, 2019.
- [24] Y. Hu, W. Kuang, Z. Qin, K. Li, J. Zhang, Y. Gao, W. Li, and K. Li, "Artificial intelligence security: threats and countermeasures," *ACM Computing Surveys (CSUR)*, vol. 55, no. 1, pp. 1–36, 2021.
- [25] A. Aldahdooh, W. Hamidouche, S. A. Fezza, and O. Déforges, "Adversarial example detection for dnn models: A review and experimental comparison," *Artificial Intelligence Review*, pp. 1–60, 2022.
- [26] G. R. Machado, E. Silva, and R. R. Goldschmidt, "Adversarial machine learning in image classification: A survey toward the defender's perspective," *ACM Computing Surveys (CSUR)*, vol. 55, no. 1, pp. 1–38, 2021.
- [27] A. Sharma, Y. Bian, P. Munz, and A. Narayan, "Adversarial patch attacks and defenses in vision-based tasks: A survey," *arXiv preprint arXiv:2206.08304*, 2022.
- [28] H. Ren, T. Huang, and H. Yan, "Adversarial examples: attacks and defenses in the physical world," *International Journal of Machine Learning and Cybernetics*, vol. 12, no. 11, pp. 3325–3336, 2021.
- [29] J. Wang, A. Liu, X. Bai, and X. Liu, "Universal adversarial patch attack for automatic checkout using perceptual and attentional bias," *IEEE Transactions on Image Processing*, vol. 31, pp. 598–611, 2021.
- [30] J. Wang, A. Liu, Z. Yin, S. Liu, S. Tang, and X. Liu, "Dual attention suppression attack: Generate adversarial camouflage in physical world," in *Proceedings of the IEEE/CVF Conference on Computer Vision and Pattern Recognition*, 2021, pp. 8565–8574.
- [31] X. Zhu, X. Li, J. Li, Z. Wang, and X. Hu, "Fooling thermal infrared pedestrian detectors in real world using small bulbs," in *Proceedings of the AAAI Conference on Artificial Intelligence*, vol. 35, no. 4, 2021, pp. 3616–3624.
- [32] X. Zhu, Z. Hu, S. Huang, J. Li, and X. Hu, "Infrared invisible clothing: Hiding from infrared detectors at multiple angles in real world," in *Proceedings of the IEEE/CVF Conference on Computer Vision and Pattern Recognition*, 2022, pp. 13 317–13 326.
- [33] D. Wang, T. Jiang, J. Sun, W. Zhou, Z. Gong, X. Zhang, W. Yao, and X. Chen, "Fca: Learning a 3d full-coverage vehicle camouflage for multi-view physical adversarial attack," in *Proceedings of the AAAI Conference on Artificial Intelligence*, vol. 36, no. 2, 2022, pp. 2414–2422.
- [34] Y. Duan, J. Chen, X. Zhou, J. Zou, Z. He, J. Zhang, W. Zhang, and Z. Pan, "Learning coated adversarial camouflages for object detectors," in *Proceedings of the Thirty-First International Joint Conference on Artificial Intelligence, IJCAI 2022, Vienna, Austria, 23-29 July 2022*, L. D. Raedt, Ed., 2022, pp. 891–897.
- [35] N. Suryanto, Y. Kim, H. Kang, H. T. Larasati, Y. Yun, T.-T.-H. Le, H. Yang, S.-Y. Oh, and H. Kim, "Dta: Physical camouflage attacks using differentiable transformation network," in *Proceedings of the IEEE/CVF Conference on Computer Vision and Pattern Recognition*, 2022, pp. 15 305–15 314.
- [36] S. Pavlitskaya, B.-M. Codău, and J. M. Zöllner, "Feasibility of inconspicuous gan-generated adversarial patches against object detection," *arXiv preprint arXiv:2207.07347*, 2022.
- [37] Y. Nemcovsky, M. Yaakoby, A. M. Bronstein, and C. Baskin, "Physical passive patch adversarial attacks on visual odometry systems," *arXiv preprint arXiv:2207.05729*, 2022.
- [38] B. G. Doan, M. Xue, S. Ma, E. Abbasnejad, and D. C. Ranasinghe, "Tnt attacks! universal naturalistic adversarial patches against deep neural network systems," *IEEE Transactions on Information Forensics and Security*, 2022.
- [39] X. Wei, Y. Guo, and J. Yu, "Adversarial sticker: A stealthy attack method in the physical world," *IEEE Transactions on Pattern Analysis and Machine Intelligence*, 2022.
- [40] X. Wei, B. Pu, J. Lu, and B. Wu, "Physically adversarial attacks and defenses in computer vision: A survey," *arXiv preprint arXiv:2211.01671*, 2022.
- [41] H. Wei, H. Tang, X. Jia, H. Yu, Z. Li, Z. Wang, S. Satoh, and Z. Wang, "Physical adversarial attack meets computer vision: A decade survey," *arXiv preprint arXiv:2209.15179*, 2022.
- [42] K. Simonyan and A. Zisserman, "Very deep convolutional networks for large-scale image recognition," *arXiv preprint arXiv:1409.1556*, 2014.
- [43] G. Huang, Z. Liu, L. Van Der Maaten, and K. Q. Weinberger, "Densely connected convolutional networks," in *Proceedings of the IEEE conference on computer vision and pattern recognition*, 2017, pp. 4700–4708.
- [44] J. Redmon, S. Divvala, R. Girshick, and A. Farhadi, "You only look once: Unified, real-time object detection," in *Proceedings of the IEEE*

- conference on computer vision and pattern recognition, 2016, pp. 779–788.
- [45] S.-T. Chen, C. Cornelius, J. Martin, and D. H. P. Chau, “Shapeshifter: Robust physical adversarial attack on faster r-cnn object detector,” in *Joint European Conference on Machine Learning and Knowledge Discovery in Databases*. Springer, 2018, pp. 52–68.
 - [46] K. Eykholt, I. Evtimov, E. Fernandes, B. Li, A. Rahmati, C. Xiao, A. Prakash, T. Kohno, and D. Song, “Robust physical-world attacks on deep learning visual classification,” in *Proceedings of the IEEE conference on computer vision and pattern recognition*, 2018, pp. 1625–1634.
 - [47] S. Thys, W. Van Ranst, and T. Goedemé, “Fooling automated surveillance cameras: adversarial patches to attack person detection,” in *Proceedings of the IEEE/CVF conference on computer vision and pattern recognition workshops*, 2019, pp. 0–0.
 - [48] L. Huang, C. Gao, Y. Zhou, C. Xie, A. L. Yuille, C. Zou, and N. Liu, “Universal physical camouflage attacks on object detectors,” in *Proceedings of the IEEE/CVF Conference on Computer Vision and Pattern Recognition*, 2020, pp. 720–729.
 - [49] A. Athalye, L. Engstrom, A. Ilyas, and K. Kwok, “Synthesizing robust adversarial examples,” in *International conference on machine learning*. PMLR, 2018, pp. 284–293.
 - [50] D. Song, K. Eykholt, I. Evtimov, E. Fernandes, B. Li, A. Rahmati, F. Tramèr, A. Prakash, and T. Kohno, “Physical adversarial examples for object detectors,” in *12th USENIX workshop on offensive technologies (WOOT 18)*, 2018.
 - [51] M. Sharif, S. Bhagavatula, L. Bauer, and M. K. Reiter, “Accessorize to a crime: Real and stealthy attacks on state-of-the-art face recognition,” in *Proceedings of the 2016 ACM SIGSAC conference on computer and communications security*, 2016, pp. 1528–1540.
 - [52] A. Mahendran and A. Vedaldi, “Understanding deep image representations by inverting them,” in *Proceedings of the IEEE conference on computer vision and pattern recognition*, 2015, pp. 5188–5196.
 - [53] S. T. Jan, J. Messou, Y.-C. Lin, J.-B. Huang, and G. Wang, “Connecting the digital and physical world: Improving the robustness of adversarial attacks,” in *Proceedings of the AAAI Conference on Artificial Intelligence*, vol. 33, no. 01, 2019, pp. 962–969.
 - [54] A. Liu, J. Wang, X. Liu, B. Cao, C. Zhang, and H. Yu, “Bias-based universal adversarial patch attack for automatic check-out,” in *European conference on computer vision*. Springer, 2020, pp. 395–410.
 - [55] A. Kurakin, I. J. Goodfellow, and S. Bengio, “Adversarial examples in the physical world,” in *5th International Conference on Learning Representations*. OpenReview.net, 2017, pp. 24–26.
 - [56] Q. Guo, F. Juefei-Xu, X. Xie, L. Ma, J. Wang, B. Yu, W. Feng, and Y. Liu, “Watch out! motion is blurry in the vision of your deep neural networks,” in *Proceedings of the 34th International Conference on Neural Information Processing Systems*, 2020, pp. 975–985.
 - [57] W. Feng, B. Wu, T. Zhang, Y. Zhang, and Y. Zhang, “Meta-attack: Class-agnostic and model-agnostic physical adversarial attack,” in *Proceedings of the IEEE/CVF International Conference on Computer Vision*, 2021, pp. 7787–7796.
 - [58] B. Phan, F. Mannan, and F. Heide, “Adversarial imaging pipelines,” in *Proceedings of the IEEE/CVF Conference on Computer Vision and Pattern Recognition*, 2021, pp. 16 051–16 061.
 - [59] T. B. Brown, D. Mané, A. Roy, M. Abadi, and J. Gilmer, “Adversarial patch,” *Advances in Neural Information Processing Systems*, 2017.
 - [60] S. Casper, M. Nadeau, D. Hadfield-Menell, and G. Kreiman, “Robust feature-level adversaries are interpretability tools,” in *Advances in Neural Information Processing Systems*, 2022.
 - [61] Y. Dong, S. Ruan, H. Su, C. Kang, X. Wei, and J. Zhu, “Viewfool: Evaluating the robustness of visual recognition to adversarial viewpoints,” in *Advances in Neural Information Processing Systems*, A. H. Oh, A. Agarwal, D. Belgrave, and K. Cho, Eds., 2022.
 - [62] N. Nichols and R. Jasper, “Projecting trouble: Light based adversarial attacks on deep learning classifiers,” *Proceedings of the AAAI Fall Symposium on Adversary-Aware Learning Techniques and Trends in Cybersecurity*, 2018.
 - [63] Y. Man, M. Li, and R. Gerdes, “Poster: Perceived adversarial examples,” in *IEEE Symposium on Security and Privacy*, no. 2019, 2019.
 - [64] A. Gnanasambandam, A. M. Sherman, and S. H. Chan, “Optical adversarial attack,” in *Proceedings of the IEEE/CVF International Conference on Computer Vision*, 2021, pp. 92–101.
 - [65] A. Sayles, A. Hooda, M. Gupta, R. Chatterjee, and E. Fernandes, “Invisible perturbations: Physical adversarial examples exploiting the rolling shutter effect,” in *Proceedings of the IEEE/CVF Conference on Computer Vision and Pattern Recognition*, 2021, pp. 14 666–14 675.
 - [66] R. Duan, X. Mao, A. K. Qin, Y. Chen, S. Ye, Y. He, and Y. Yang, “Adversarial laser beam: Effective physical-world attack to dnn in a blink,” in *Proceedings of the IEEE/CVF Conference on Computer Vision and Pattern Recognition*, 2021, pp. 16 062–16 071.
 - [67] K. Kim, J. Kim, S. Song, J.-H. Choi, C. Joo, and J.-S. Lee, “Light lies: Optical adversarial attack,” *arXiv preprint arXiv:2106.09908*, 2021.
 - [68] B. Huang and H. Ling, “Spaa: Stealthy projector-based adversarial attacks on deep image classifiers,” in *2022 IEEE Conference on Virtual Reality and 3D User Interfaces (VR)*. IEEE, 2022, pp. 534–542.
 - [69] M. Sharif, S. Bhagavatula, L. Bauer, and M. K. Reiter, “A general framework for adversarial examples with objectives,” *ACM Transactions on Privacy and Security (TOPS)*, vol. 22, no. 3, pp. 1–30, 2019.
 - [70] I. Singh, S. Momiyama, K. Kakizaki, and T. Araki, “On brightness agnostic adversarial examples against face recognition systems,” in *2021 International Conference of the Biometrics Special Interest Group (BIOSIG)*. IEEE, 2021, pp. 1–5.
 - [71] B. Zhang, B. Tondi, and M. Barni, “Adversarial examples for replay attacks against cnn-based face recognition with anti-spoofing capability,” *Computer Vision and Image Understanding*, vol. 197, p. 102988, 2020.
 - [72] M. Pautov, G. Melnikov, E. Kaziakhmedov, K. Kireev, and A. Petiushko, “On adversarial patches: real-world attack on arcfacel-100 face recognition system,” in *2019 International Multi-Conference on Engineering, Computer and Information Sciences (SIBIRCON)*. IEEE, 2019, pp. 0391–0396.
 - [73] S. Komkov and A. Petiushko, “Advhat: Real-world adversarial attack on arcfacel face id system,” in *2020 25th International Conference on Pattern Recognition (ICPR)*. IEEE, 2021, pp. 819–826.
 - [74] Z. Xiao, X. Gao, C. Fu, Y. Dong, W. Gao, X. Zhang, J. Zhou, and J. Zhu, “Improving transferability of adversarial patches on face recognition with generative models,” in *Proceedings of the IEEE/CVF Conference on Computer Vision and Pattern Recognition*, 2021, pp. 11 845–11 854.
 - [75] X. Wei, Y. Guo, J. Yu, and B. Zhang, “Simultaneously optimizing perturbations and positions for black-box adversarial patch attacks,” *arXiv preprint arXiv:2212.12995*, 2022.
 - [76] A. Zolfi, S. Avidan, Y. Elovici, and A. Shabtai, “Adversarial mask: Real-world adversarial attack against face recognition models,” 2022.
 - [77] D.-L. Nguyen, S. S. Arora, Y. Wu, and H. Yang, “Adversarial light projection attacks on face recognition systems: A feasibility study,” in *Proceedings of the IEEE/CVF conference on computer vision and pattern recognition workshops*, 2020, pp. 814–815.
 - [78] C. Sitawarin, A. N. Bhagoji, A. Mosenia, P. Mittal, and M. Chiang, “Rogue signs: Deceiving traffic sign recognition with malicious ads and logos,” *arXiv preprint arXiv:1801.02780*, 2018.
 - [79] A. Liu, X. Liu, J. Fan, Y. Ma, A. Zhang, H. Xie, and D. Tao, “Perceptual-sensitive gan for generating adversarial patches,” in *Proceedings of the AAAI conference on artificial intelligence*, vol. 33, no. 01, 2019, pp. 1028–1035.
 - [80] R. Duan, X. Ma, Y. Wang, J. Bailey, A. K. Qin, and Y. Yang, “Adversarial camouflage: Hiding physical-world attacks with natural styles,” in *Proceedings of the IEEE/CVF conference on computer vision and pattern recognition*, 2020, pp. 1000–1008.
 - [81] Y. Zhong, X. Liu, D. Zhai, J. Jiang, and X. Ji, “Shadows can be dangerous: Stealthy and effective physical-world adversarial attack by natural phenomenon,” in *Proceedings of the IEEE/CVF Conference on Computer Vision and Pattern Recognition*, 2022, pp. 15 345–15 354.
 - [82] Z. Wang, S. Zheng, M. Song, Q. Wang, A. Rahimpour, and H. Qi, “advpattern: physical-world attacks on deep person re-identification via adversarially transformable patterns,” in *Proceedings of the IEEE/CVF International Conference on Computer Vision*, 2019, pp. 8341–8350.
 - [83] Z. Kong, J. Guo, A. Li, and C. Liu, “Physgan: Generating physical-world-resilient adversarial examples for autonomous driving,” in *Proceedings of the IEEE/CVF Conference on Computer Vision and Pattern Recognition*, 2020, pp. 14 254–14 263.
 - [84] Y. Qian, D. Ma, B. Wang, J. Pan, J. Wang, Z. Gu, J. Chen, W. Zhou, and J. Lei, “Spot evasion attacks: Adversarial examples for license plate recognition systems with convolutional neural networks,” *Computers & Security*, vol. 95, p. 101826, 2020.
 - [85] Y. Zhao, H. Zhu, R. Liang, Q. Shen, S. Zhang, and K. Chen, “Seeing isn’t believing: Towards more robust adversarial attack against real world object detectors,” in *Proceedings of the 2019 ACM SIGSAC Conference on Computer and Communications Security*, 2019, pp. 1989–2004.
 - [86] M. Lee and Z. Kolter, “On physical adversarial patches for object detection,” *arXiv preprint arXiv:1906.11897*, 2019.

- [87] K. Yang, T. Tsai, H. Yu, T.-Y. Ho, and Y. Jin, "Beyond digital domain: Fooling deep learning based recognition system in physical world," in *Proceedings of the AAAI Conference on Artificial Intelligence*, vol. 34, no. 01, 2020, pp. 1088–1095.
- [88] A. Zolfi, M. Kravchik, Y. Elovici, and A. Shabtai, "The translucent patch: A physical and universal attack on object detectors," in *Proceedings of the IEEE/CVF Conference on Computer Vision and Pattern Recognition*, 2021, pp. 15 232–15 241.
- [89] A. Shapira, R. Bitton, D. Avraham, A. Zolfi, Y. Elovici, and A. Shabtai, "Attacking object detector using a universal targeted label-switch patch," *arXiv preprint arXiv:2211.08859*, 2022.
- [90] S. Hoory, T. Shapira, A. Shabtai, and Y. Elovici, "Dynamic adversarial patch for evading object detection models," *arXiv preprint arXiv:2010.13070*, 2020.
- [91] D. Y. Yang, J. Xiong, X. Li, X. Yan, J. Raiti, Y. Wang, H. Wu, and Z. Zhong, "Building towards" invisible cloak": Robust physical adversarial attack on yolo object detector," in *2018 9th IEEE Annual Ubiquitous Computing, Electronics & Mobile Communication Conference (UEMCON)*. IEEE, 2018, pp. 368–374.
- [92] K. Xu, G. Zhang, S. Liu, Q. Fan, M. Sun, H. Chen, P.-Y. Chen, Y. Wang, and X. Lin, "Adversarial t-shirt! evading person detectors in a physical world," in *European conference on computer vision*. Springer, 2020, pp. 665–681.
- [93] Z. Wu, S.-N. Lim, L. S. Davis, and T. Goldstein, "Making an invisibility cloak: Real world adversarial attacks on object detectors," in *European Conference on Computer Vision*. Springer, 2020, pp. 1–17.
- [94] J. Tan, N. Ji, H. Xie, and X. Xiang, "Legitimate adversarial patches: Evading human eyes and detection models in the physical world," in *Proceedings of the 29th ACM International Conference on Multimedia*, 2021, pp. 5307–5315.
- [95] Y.-C.-T. Hu, B.-H. Kung, D. S. Tan, J.-C. Chen, K.-L. Hua, and W.-H. Cheng, "Naturalistic physical adversarial patch for object detectors," in *Proceedings of the IEEE/CVF International Conference on Computer Vision*, 2021, pp. 7848–7857.
- [96] Z. Hu, S. Huang, X. Zhu, F. Sun, B. Zhang, and X. Hu, "Adversarial texture for fooling person detectors in the physical world," in *Proceedings of the IEEE/CVF Conference on Computer Vision and Pattern Recognition*, 2022, pp. 13 307–13 316.
- [97] G. Lovisotto, H. Turner, I. Sluganovic, M. Strohmeier, and I. Martinovic, "Slap: Improving physical adversarial examples with short-lived adversarial perturbations," in *30th USENIX Security Symposium (USENIX Security 21)*, 2021, pp. 1865–1882.
- [98] X. Zeng, C. Liu, Y.-S. Wang, W. Qiu, L. Xie, Y.-W. Tai, C.-K. Tang, and A. L. Yuille, "Adversarial attacks beyond the image space," in *Proceedings of the IEEE/CVF Conference on Computer Vision and Pattern Recognition*, 2019, pp. 4302–4311.
- [99] Y. Zhang, P. H. Foroosh, and B. Gong, "Camou: Learning a vehicle camouflage for physical adversarial attack on object detections in the wild," *ICLR*, 2019.
- [100] T. Wu, X. Ning, W. Li, R. Huang, H. Yang, and Y. Wang, "Physical adversarial attack on vehicle detector in the carla simulator," *arXiv preprint arXiv:2007.16118*, 2020.
- [101] A. Du, B. Chen, T.-J. Chin, Y. W. Law, M. Sasdelli, R. Rajasegaran, and D. Campbell, "Physical adversarial attacks on an aerial imagery object detector," in *Proceedings of the IEEE/CVF Winter Conference on Applications of Computer Vision*, 2022, pp. 1796–1806.
- [102] F. Nesti, G. Rossolini, S. Nair, A. Biondi, and G. Buttazzo, "Evaluating the robustness of semantic segmentation for autonomous driving against real-world adversarial patch attacks," in *Proceedings of the IEEE/CVF Winter Conference on Applications of Computer Vision*, 2022, pp. 2280–2289.
- [103] Z. Cheng, J. Liang, H. Choi, G. Tao, Z. Cao, D. Liu, and X. Zhang, "Physical attack on monocular depth estimation with optimal adversarial patches," in *European Conference on Computer Vision*. Springer, 2022, pp. 514–532.
- [104] R. R. Wiyatno and A. Xu, "Physical adversarial textures that fool visual object tracking," in *Proceedings of the IEEE/CVF International Conference on Computer Vision*, 2019, pp. 4822–4831.
- [105] L. Ding, Y. Wang, K. Yuan, M. Jiang, P. Wang, H. Huang, and Z. J. Wang, "Towards universal physical attacks on single object tracking," in *AAAI*, 2021, pp. 1236–1245.
- [106] P. Isola, J.-Y. Zhu, T. Zhou, and A. A. Efros, "Image-to-image translation with conditional adversarial networks," in *Proceedings of the IEEE conference on computer vision and pattern recognition*, 2017, pp. 1125–1134.
- [107] J.-Y. Zhu, T. Park, P. Isola, and A. A. Efros, "Unpaired image-to-image translation using cycle-consistent adversarial networks," in *Proceedings of the IEEE international conference on computer vision*, 2017, pp. 2223–2232.
- [108] M. Jaderberg, K. Simonyan, A. Zisserman *et al.*, "Spatial transformer networks," *Advances in neural information processing systems*, vol. 28, 2015.
- [109] C. Xiao, B. Li, J.-Y. Zhu, W. He, M. Liu, and D. Song, "Generating adversarial examples with adversarial networks," in *Proceedings of the 27th International Joint Conference on Artificial Intelligence*, 2018, p. 3905–3911.
- [110] Z.-A. Zhu, Y.-Z. Lu, and C.-K. Chiang, "Generating adversarial examples by makeup attacks on face recognition," in *2019 IEEE International Conference on Image Processing (ICIP)*. IEEE, 2019, pp. 2516–2520.
- [111] T. Malzbender, D. Gelb, and H. Wolters, "Polynomial texture maps," in *Proceedings of the 28th annual conference on Computer graphics and interactive techniques*, 2001, pp. 519–528.
- [112] R. R. Selvaraju, M. Cogswell, A. Das, R. Vedantam, D. Parikh, and D. Batra, "Grad-cam: Visual explanations from deep networks via gradient-based localization," in *Proceedings of the IEEE international conference on computer vision*, 2017, pp. 618–626.
- [113] L. A. Gatys, A. S. Ecker, and M. Bethge, "Image style transfer using convolutional neural networks," in *Proceedings of the IEEE conference on computer vision and pattern recognition*, 2016, pp. 2414–2423.
- [114] J. Redmon and A. Farhadi, "Yolov3: An incremental improvement," *arXiv preprint arXiv:1804.02767*, 2018.
- [115] W. Liu, D. Anguelov, D. Erhan, C. Szegedy, S. Reed, C.-Y. Fu, and A. C. Berg, "Ssd: Single shot multibox detector," in *European conference on computer vision*. Springer, 2016, pp. 21–37.
- [116] T.-Y. Lin, P. Goyal, R. Girshick, K. He, and P. Dollár, "Focal loss for dense object detection," in *Proceedings of the IEEE international conference on computer vision*, 2017, pp. 2980–2988.
- [117] S. Ren, K. He, R. Girshick, and J. Sun, "Faster r-cnn: Towards real-time object detection with region proposal networks," *Advances in neural information processing systems*, vol. 28, pp. 91–99, 2015.
- [118] K. He, G. Gkioxari, P. Dollár, and R. Girshick, "Mask r-cnn," in *Proceedings of the IEEE international conference on computer vision*, 2017, pp. 2961–2969.
- [119] X. Liu, H. Yang, Z. Liu, L. Song, H. Li, and Y. Chen, "Dpatch: An adversarial patch attack on object detectors," *arXiv preprint arXiv:1806.02299*, 2018.
- [120] T.-Y. Lin, P. Dollár, R. Girshick, K. He, B. Hariharan, and S. Belongie, "Feature pyramid networks for object detection," in *Proceedings of the IEEE conference on computer vision and pattern recognition*, 2017, pp. 2117–2125.
- [121] X. Yang, F. Wei, H. Zhang, and J. Zhu, "Design and interpretation of universal adversarial patches in face detection," in *European Conference on Computer Vision*. Springer, 2020, pp. 174–191.
- [122] C. Xiao, D. Yang, B. Li, J. Deng, and M. Liu, "Meshadv: Adversarial meshes for visual recognition," in *Proceedings of the IEEE/CVF Conference on Computer Vision and Pattern Recognition*, 2019, pp. 6898–6907.
- [123] A. Dosovitskiy, G. Ros, F. Codevilla, A. Lopez, and V. Koltun, "Carla: An open urban driving simulator," in *Conference on robot learning*. PMLR, 2017, pp. 1–16.
- [124] Z. Li, C. Peng, G. Yu, X. Zhang, Y. Deng, and J. Sun, "Light-head r-cnn: In defense of two-stage object detector," *arXiv preprint arXiv:1711.07264*, 2017.
- [125] H. Kato, Y. Ushiku, and T. Harada, "Neural 3d mesh renderer," in *Proceedings of the IEEE conference on computer vision and pattern recognition*, 2018, pp. 3907–3916.
- [126] M. Tan, R. Pang, and Q. V. Le, "Efficientdet: Scalable and efficient object detection," in *Proceedings of the IEEE/CVF conference on computer vision and pattern recognition*, 2020, pp. 10 781–10 790.
- [127] J. Byun, S. Cho, M.-J. Kwon, H.-S. Kim, and C. Kim, "Improving the transferability of targeted adversarial examples through object-based diverse input," in *Proceedings of the IEEE/CVF Conference on Computer Vision and Pattern Recognition*, 2022, pp. 15 244–15 253.
- [128] M. A. Alcorn, Q. Li, Z. Gong, C. Wang, L. Mai, W.-S. Ku, and A. Nguyen, "Strike (with) a pose: Neural networks are easily fooled by strange poses of familiar objects," in *Proceedings of the IEEE/CVF Conference on Computer Vision and Pattern Recognition*, 2019, pp. 4845–4854.
- [129] R. den Hollander, A. Adhikari, I. Tolios, M. van Bekkum, A. Bal, S. Hendriks, M. Kruithof, D. Gross, N. Jansen, G. Perez *et al.*, "Adversarial patch camouflage against aerial detection," in *Artificial Intelligence and Machine Learning in Defense Applications II*, vol. 11543. SPIE, 2020, pp. 77–86.

- [130] L. Chen, G. Zhu, Q. Li, and H. Li, "Adversarial example in remote sensing image recognition," *arXiv preprint arXiv:1910.13222*, 2019.
- [131] L. Chen, H. Li, G. Zhu, Q. Li, J. Zhu, H. Huang, J. Peng, and L. Zhao, "Attack selectivity of adversarial examples in remote sensing image scene classification," *IEEE Access*, vol. 8, pp. 137 477–137 489, 2020.
- [132] Y. Xu, B. Du, and L. Zhang, "Assessing the threat of adversarial examples on deep neural networks for remote sensing scene classification: Attacks and defenses," *IEEE Transactions on Geoscience and Remote Sensing*, vol. 59, no. 2, pp. 1604–1617, 2020.
- [133] Y. Wang, K. Wang, Z. Zhu, and F.-Y. Wang, "Adversarial attacks on faster r-cnn object detector," *Neurocomputing*, vol. 382, pp. 87–95, 2020.
- [134] K.-H. Chow, L. Liu, M. Loper, J. Bae, M. E. Gursoy, S. Truex, W. Wei, and Y. Wu, "Adversarial objectness gradient attacks in real-time object detection systems," in *2020 Second IEEE International Conference on Trust, Privacy and Security in Intelligent Systems and Applications (TPS-ISA)*. IEEE, 2020, pp. 263–272.
- [135] D. Wang, C. Li, S. Wen, Q.-L. Han, S. Nepal, X. Zhang, and Y. Xiang, "Daedalus: Breaking nonmaximum suppression in object detection via adversarial examples," *IEEE Transactions on Cybernetics*, 2021.
- [136] Q. Liao, X. Wang, B. Kong, S. Lyu, Y. Yin, Q. Song, and X. Wu, "Fast local attack: Generating local adversarial examples for object detectors," in *2020 International Joint Conference on Neural Networks (IJCNN)*. IEEE, 2020, pp. 1–8.
- [137] J. Bao, "Sparse adversarial attack to object detection," *arXiv preprint arXiv:2012.13692*, 2020.
- [138] S. Wu, T. Dai, and S.-T. Xia, "Dpattack: Diffused patch attacks against universal object detection," *arXiv preprint arXiv:2010.11679*, 2020.
- [139] H. Huang, Y. Wang, Z. Chen, Z. Tang, W. Zhang, and K.-K. Ma, "Rpattack: Refined patch attack on general object detectors," in *2021 IEEE International Conference on Multimedia and Expo (ICME)*. IEEE, 2021, pp. 1–6.
- [140] N. Papernot, P. McDaniel, S. Jha, M. Fredrikson, Z. B. Celik, and A. Swami, "The limitations of deep learning in adversarial settings," in *2016 IEEE European symposium on security and privacy (EuroS&P)*. IEEE, 2016, pp. 372–387.
- [141] F. Croce and M. Hein, "Sparse and imperceivable adversarial attacks," in *Proceedings of the IEEE/CVF International Conference on Computer Vision*, 2019, pp. 4724–4732.
- [142] A. Modas, S.-M. Moosavi-Dezfooli, and P. Frossard, "Sparsefool: a few pixels make a big difference," in *Proceedings of the IEEE/CVF conference on computer vision and pattern recognition*, 2019, pp. 9087–9096.
- [143] X. Dong, D. Chen, J. Bao, C. Qin, L. Yuan, W. Zhang, N. Yu, and D. Chen, "Greedyfool: Distortion-aware sparse adversarial attack," *Advances in Neural Information Processing Systems*, vol. 33, pp. 11 226–11 236, 2020.
- [144] Z. He, W. Wang, J. Dong, and T. Tan, "Transferable sparse adversarial attack," in *Proceedings of the IEEE/CVF Conference on Computer Vision and Pattern Recognition*, 2022, pp. 14 963–14 972.
- [145] Y. Zhao, H. Yan, and X. Wei, "Object hider: Adversarial patch attack against object detectors," *arXiv preprint arXiv:2010.14974*, 2020.
- [146] D. Li, J. Zhang, and K. Huang, "Universal adversarial perturbations against object detection," *Pattern Recognition*, vol. 110, p. 107584, 2021.
- [147] S.-M. Moosavi-Dezfooli, A. Fawzi, O. Fawzi, and P. Frossard, "Universal adversarial perturbations," in *Proceedings of the IEEE conference on computer vision and pattern recognition*, 2017, pp. 1765–1773.
- [148] Z. Zhu, H. Su, C. Liu, W. Xiang, and S. Zheng, "You cannot easily catch me: A low-detectable adversarial patch for object detectors," *arXiv preprint arXiv:2109.15177*, 2021.
- [149] Y. Cao, C. Xiao, B. Cyr, Y. Zhou, W. Park, S. Rampazzi, Q. A. Chen, K. Fu, and Z. M. Mao, "Adversarial sensor attack on lidar-based perception in autonomous driving," in *Proceedings of the 2019 ACM SIGSAC conference on computer and communications security*, 2019, pp. 2267–2281.
- [150] T. Sato, J. Shen, N. Wang, Y. Jia, X. Lin, and Q. A. Chen, "Dirty road can attack: Security of deep learning based automated lane centering under {Physical-World} attack," in *30th USENIX Security Symposium (USENIX Security 21)*, 2021, pp. 3309–3326.
- [151] J. Tu, H. Li, X. Yan, M. Ren, Y. Chen, M. Liang, E. Bitar, E. Yumer, and R. Urtasun, "Exploring adversarial robustness of multi-sensor perception systems in self driving," *arXiv preprint arXiv:2101.06784*, 2021.
- [152] J. Hendrik Metzen, M. Chaithanya Kumar, T. Brox, and V. Fischer, "Universal adversarial perturbations against semantic image segmentation," in *Proceedings of the IEEE international conference on computer vision*, 2017, pp. 2755–2764.
- [153] K. K. Nakka and M. Salzmann, "Indirect local attacks for context-aware semantic segmentation networks," in *European Conference on Computer Vision*. Springer, 2020, pp. 611–628.
- [154] A. Arnab, O. Miksik, and P. H. Torr, "On the robustness of semantic segmentation models to adversarial attacks," in *Proceedings of the IEEE Conference on Computer Vision and Pattern Recognition*, 2018, pp. 888–897.
- [155] M. Alzantot, Y. Sharma, S. Chakraborty, H. Zhang, C.-J. Hsieh, and M. B. Srivastava, "Genattack: Practical black-box attacks with gradient-free optimization," in *Proceedings of the Genetic and Evolutionary Computation Conference*, 2019, pp. 1111–1119.
- [156] M. Andriushchenko, F. Croce, N. Flammarion, and M. Hein, "Square attack: a query-efficient black-box adversarial attack via random search," in *European Conference on Computer Vision*. Springer, 2020, pp. 484–501.
- [157] C. Li, W. Yao, H. Wang, and T. Jiang, "Adaptive momentum variance for attention-guided sparse adversarial attacks," *Pattern Recognition*, vol. 133, p. 108979, 2023.
- [158] A. Ghosh, S. S. Mullick, S. Datta, S. Das, A. K. Das, and R. Mallipeddi, "A black-box adversarial attack strategy with adjustable sparsity and generalizability for deep image classifiers," *Pattern Recognition*, vol. 122, p. 108279, 2022.
- [159] A. Dosovitskiy, G. Ros, F. Codevilla, A. Lopez, and V. Koltun, "CARLA: An open urban driving simulator," in *Proceedings of the 1st Annual Conference on Robot Learning*, 2017, pp. 1–16.
- [160] S. Shah, D. Dey, C. Lovett, and A. Kapoor, "Airsim: High-fidelity visual and physical simulation for autonomous vehicles," in *Field and Service Robotics*, 2017. [Online]. Available: <https://arxiv.org/abs/1705.05065>
- [161] H. Salman, A. Ilyas, L. Engstrom, S. Vemprala, A. Madry, and A. Kapoor, "Unadversarial examples: Designing objects for robust vision," *Advances in Neural Information Processing Systems*, vol. 34, pp. 15 270–15 284, 2021.
- [162] J. Wang, Z. Yin, P. Hu, A. Liu, R. Tao, H. Qin, X. Liu, and D. Tao, "Defensive patches for robust recognition in the physical world," in *Proceedings of the IEEE/CVF Conference on Computer Vision and Pattern Recognition*, 2022, pp. 2456–2465.